Octopamine neurons mediate flight-induced modulation of visual processing in *Drosophila melanogaster*

Thesis by

Marie P. Suver

In Partial Fulfillment of the Requirements

for the Degree of

Doctor of Philosophy

California Institute of Technology

Pasadena, California

2014

(Defended June 13, 2013)

In memory of my grandmother, Patricia Louise Staggs.

Acknowledgments

First I would like to thank my advisor Michael Dickinson, whose advice and support over the years I am grateful for. Michael inspires a thoughtful, creative and rigorous approach to science and I am incredibly fortunate to have spent this time in his lab.

I would also like to thank my committee members for their useful comments, criticisms and time: Thanos Siapas, Pietro Perona, Paul Sternberg, and Markus Meister. Thanks to David Anderson for input over the years as well.

Akira Mamiya performed the calcium imaging experiments presented in Chapter 2, and tested many exciting theories about the effect of wind stimuli and visual responses in octopamine neurons not presented here. I owe a huge thanks to Anne Sustar, who provided the image of the *Tdc2-Gal4* line presented in Chapter 2, offered expert help and advice for acquiring genetic reagents, setting up crosses, and immunohistochemistry procedures.

I am also very grateful to Dr. Edward Kravitz and the members of his lab who provided the octopamine Gal4 driver lines presented in Chapter 3. Dr. Bun Chan generated the octopamine neuron enhancer trap lines, and Dr. Kyle Gobrogge generated a number of effector lines for single cell manipulations and was a consistently cheery and helpful collaborator.

Thanks to Floris van Breugel, who performed the free flight experiments discussed in the conclusion with great enthusiasm. Thanks also to Bettina Schnell, who aided in the design of these free flight experiments, and whose no-fuss approach to electrophysiology is always refreshing.

I would also like to thank my friend and colleague Peter Weir, for lively discussions, collaborations, and great company.

Abstract

Activity-dependent modulation of sensory systems has been documented in many organisms, and is likely to be essential for appropriate processing of information during different behavioral states. However, the mechanisms underlying these phenomena, and often their functional consequences, remain poorly characterized. I investigated the role of octopamine neurons in the flight-dependent modulation observed in visual interneurons in the fruit fly *Drosophila melanogaster*. The vertical system (VS) cells exhibit a boost in their response to visual motion during flight compared to quiescence. Pharmacological application of octopamine evokes responses in quiescent flies that mimic those observed during flight, and octopamine neurons that project to the optic lobes increase in activity during flight. Using genetic tools to manipulate the activity of octopamine neurons, I find that they are both necessary and sufficient for the flight-induced visual boost. This work provides the first evidence that endogenous release of octopamine is involved in state-dependent modulation of visual interneurons in flies. Further, I investigated the role of a single pair of octopamine neurons that project to the optic lobes, and found no evidence that chemical synaptic transmission via these neurons is necessary for the flight boost. However, I found some evidence that activation of these neurons may contribute to the flight boost. Wind stimuli alone are sufficient to generate transient increases in the VS cell response to motion vision, but result in no increase in baseline membrane potential. These results suggest that the flight boost originates not from a central command signal during flight, but from mechanosensory stimuli relayed via the octopamine system. Lastly, in an attempt to understand the functional consequences of the flight boost observed in visual interneurons, we measured the effect of inactivating octopamine neurons in freely

flying flies. We found that flies whose octopamine neurons we silenced accelerate less than wild-type flies, consistent with the hypothesis that the flight boost we observe in VS cells is indicative of a gain control mechanism mediated by octopamine neurons. Together, this work serves as the basis for a mechanistic and functional understanding of octopaminergic modulation of vision in flying flies.

Contents

List of Figures

List of Tables

Chapter 1

Introduction

A key feature of nervous systems is the ability to process sensory stimuli in a context-dependent manner. For example, it has been shown in mice that the responses of neurons in primary visual cortex increase during locomotion (Andermann et al., 2011; Niell and Stryker, 2010), and this effect is reminiscent of the modulation observed when a monkey attends to a stimulus (Moran and Desimone, 1985; Treue and Maunsell, 1996). Similarly, the responses of visual interneurons in flies are enhanced during walking (Chiappe et al., 2010) and flight (Maimon et al., 2010; Jung et al., 2011), compared to the responses in quiescent flies. Given these similar observations in flies, mice and primates, state-dependent sensory modulation is likely to be quite general, although the cellular mechanisms underlying such changes are not known. Given the relatively small number of neurons in the *Drosophila* brain and the abundance of genetic tools available with which to manipulate neural activity, the fruit fly provides an excellent model system to probe the cellular and molecular basis of behavioral modulation of sensory systems.

1.1 The visual system of the fly

Flies rely on vision for many tasks, including finding mates, traveling long distances in the absence of visual landmarks (Coyne et al., 1982), and avoiding obstacles and predators. They have evolved the fastest visual system in the animal kingdom (Autrum, 1958), and roughly one half of the brain is dedicated to visual processing

(Rein et al., 2002). The fly visual system has been a subject of intense study for nearly a century, from the elegant anatomical characterization by Cajal and Sanchez (1915) to modern neurogenetics. Indeed, for those interested in unraveling the neural basis of behavior, vision and its role in fly behavior presents a rich yet relatively accessible system.

Adult flies use two sensory structures to detect light - the compound eyes and the ocelli. The ocelli are a set of three simple eyes positioned on the top (dorsal[1]-most part) of the head, and are believed to aid in gaze stabilization (Goodman, 1970; Schuppe and Hengstenberg, 1993). Ocellar interneurons, called L-neurons, sum information from photoreceptor outputs in each of the ocelli, and form a low-resolution image of the visual world. These large diameter neurons rapidly relay intensity information to the posterior slope, where they synapse onto descending neurons (Nässel and Hagberg, 1985; Strausfeld, 1976; Strausfeld and Bassemir, 1985) and possibly the large motion sensitive neurons of the third optic neuropil (Parsons et al., 2010; Strausfeld, 1976). Most of the neurons in the visual system, however, are dedicated to processing information from the compound eyes, where light is first detected by the retina. The retina of each eye in *Drosophila* consists of an array of about 700 ommatidia (Heisenberg et al., 1984), specialized light-sensing structures in which photoreceptors are housed (Figure 1.1). Visual information is retinotopically projected from the retina to a series of neuropil in which subsequent computations are performed: the lamina, medulla, and the lobula complex, which consists of the lobula and the lobula plate (Figure 1.1).

Using a variety of techniques, including electrophysiology, genetic manipulation, and behavioral analysis, researchers have started to unravel the cellular basis of the earliest stages of motion processing (Clark et al., 2011; Eichner et al., 2011). Visual motion processing in the fly begins with the so-called elementary motion detectors (EMDs), which are units sensitive to one direction of motion over a small receptive

---

[1]Some researchers prefer to report brain anatomy relative to the neuraxis, which is an anatomical reference system based on development, and is especially helpful in comparative studies (a useful figure can be found in Strausfeld and Seyan, 1985). However, the work presented in this thesis focuses on a single species, and so I have chosen to refer to brain anatomy relative to the body axis for clarity.

Figure 1.1: Major brain regions of the *Drosophila* optic lobes. A horizontal section of the head reveals major neuropil in the optic lobes, labeled in white. Also labeled are a single ommatidium, and the posterior slope, where some of the wide field motion sensitive neurons of the lobula plate project to. Image from the Fischbach lab (http://brain.biologie.uni-freiburg.de/Atlas/text/paraffinFi.html, modified).

field (Buchner, 1976, 1984; Hassenstein and Reichardt, 1956). The identities of the cells involved in this computation are under active research, and a complete picture has yet to emerge (Clark et al., 2011; Eichner et al., 2011).

Partly due to the accessibility of a set of large interneurons located in the lobula plate, we know a great deal more about higher order visual processing than the early stages of motion processing. There are nearly two dozen classes of lobula plate tangential cells (LPTCs), which are neurons distinguished by their large characteristic dendrites and sensitivity to wide-field motion (Hausen, 1984; Hengstenberg et al., 1982). Forty years ago, the vertical system (VS) and horizontal system (HS) cells were discovered (Braitenberg, 1972) and have since become some of the most widely studied neurons in the insect visual system . First named for their conspicuous vertical and horizontal dendritic arbors (Pierantoni, 1973, also see Figure 1.2), the vertical and horizontal system cells were later found to respond to motion in the vertical and horizontal directions, respectively (Braitenberg, 1972; Dvorak et al., 1975; Hausen, 1976, 1984). Their axonal responses are graded changes in membrane potential;

VS and HS cells depolarize in response to motion in their preferred direction, and hyperpolarize in response to non-preferred (null direction) motion. Although they do not typically fire action potentials, they produce small, regenerative spike-like events (Hengstenberg 1977, Figure 1.3).
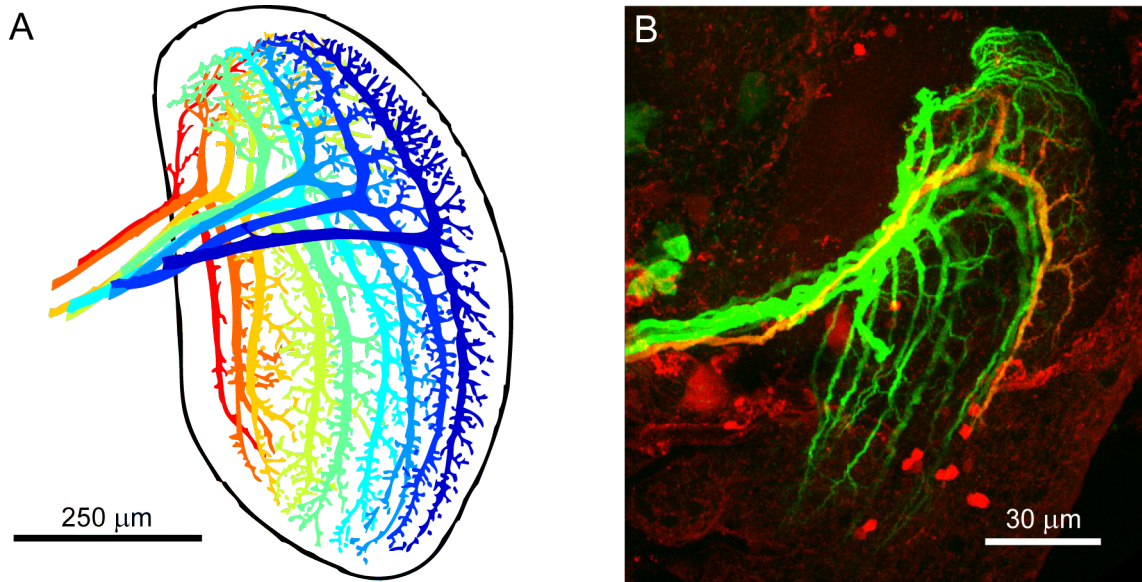
Figure 1.2: Anatomy of VS cell dendrites. (A) Reconstruction of nine VS cells in *Calliphora erythrocephala* (there are thought to be up to 11 VS cells in this species of fly). Each VS cell is depicted in a different color within the lobula plate (outline in black). Cell bodies and axon terminals not shown. Modified from Hengstenberg et al. (1982). (B) Confocal image of the six VS cells in *Drosophila melanogaster* labeled with green fluorescent protein (GFP, green), with VS1 (filled with biocytin hydrazide during one of my recordings, shown in red) overlaid. The VS cells were labeled using the Janelia Farm Gal4 driver line *R78F01-Gal4* expressing GFP. This driver line also labels a non-VS cell with fine processes in the lobula plate just beyond the most anterior region of the VS dendrites. Some VS cell bodies can be seen near the axonal tract towards the left of the image. The cell body of the filled neuron was removed when the recording electrode was lifted away from the preparation. Both (A) and (B) show a frontal view of VS processes in the right lobula plate, and the top of each image is most anterior.

The motion sensitivity of the VS and HS cells arises from the integration of direct input from a retinotopic array of excitatory and inhibitory EMDs (Borst et al., 1995). Anatomical (Bausenwein et al., 1992) and physiological evidence (Schnell et al., 2012) support that T4 and T5 cells provide directionally selective input to the VS and HS cells. T4 and T5 cells receive input from the 'on' and 'off' motion pathways, via the L1
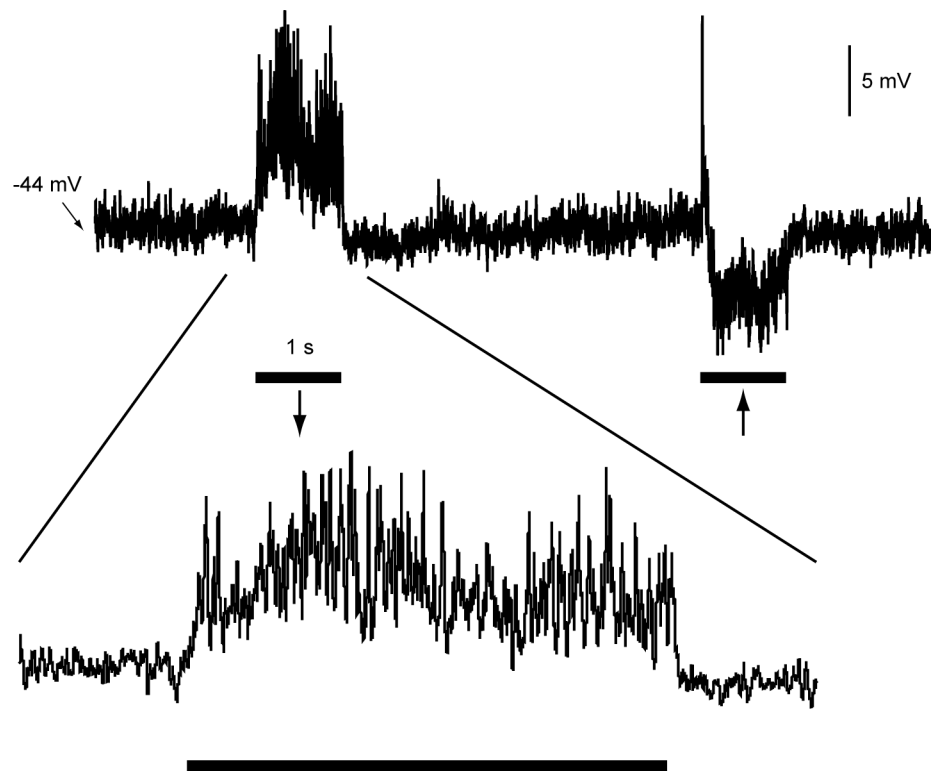
Figure 1.3: Typical VS cell response to visual motion. This trace shows the raw membrane potential of a VS3 cell during rest and in response to motion. Black bars indicate when stimulus was in motion. The stimulus was a 1 Hz graded sine wave grating moving downward (preferred direction, down arrow) or upward (null direction, up arrow). The expanded trace shows the small spike-like events that are typical of these cells.

and L2 neurons in the medulla and lobula, respectively (Joesch et al., 2010). Subsets of T4 and T5 neurons each project to the four layers of the lobula plate, which are believed to process visual motion in four different directions (Buchner et al., 1984). VS and HS cells were initially thought to be most sensitive to movement in restricted fields of view, based on this retinotopic input. However, later studies showed that VS cells are responsive to motion across large regions in both the ipsilateral and contralateral visual fields, and respond best to motion that corresponds to the optic flow generated by the fly rotating about different body axes (Krapp and Hengstenberg, 1996).

For some time it was unclear how the receptive fields of VS and HS cells arise, given the anatomically limited range of their dendritic arbors. How does information

from outside the receptive field of areas covered by the dendrites of a VS cell affect its axonal membrane potential? By using paired recordings, researchers demonstrated that VS, HS and another class of LPTCs, the two centrifugal horizontal (CH) cells (Hausen, 1976), are connected via gap junctions into a network in which neighboring cells excite each other, broadening and tuning the receptive field of each (Haag and Borst, 2004, 2005). Both electrophysiological experiments and dye coupling results suggest that HS and CH cells make dendro-dendritic contacts, and each VS cell is electrically coupled to its immediate neighbor(s) (Haag and Borst, 2004, 2005). The rotational sensitivity of these cells is now attributed in part to the tuning properties of their inputs and in part to the connectivity pattern within the network.

An additional mechanism appears to contribute to the rotational tuning of these cells at the level of the dendrites. Elyada et al. (2013) recently monitored activity in the dendrites of VS and HS cells with a calcium-sensitive dye. They reported a previously unknown phenomenon at work, termed "end inhibition," which consists of a decrease in dendritic responses when patterns are extended in the direction perpendicular to a cell's preferred direction of motion. Thus, the responses in the dendrites of a VS cell, sensitive to vertical motion, decrease when the same vertically moving pattern is made wider. This inhibition in the dendrites contrasts with the behavior at the axon of the same cell: because of gap junctions with neighboring VS cells, axonal responses increase when stimulus patterns extend over a wider horizontal area. These effects are illustrated in Figure 1.4. The authors suggest that the inhibitory input from upstream EMDs outside the VS cell's excitatory receptive field are likely candidates for the source of this inhibition, based on experiments in which they injected current while stimulating VS cells with patterns of different widths (red curved inhibitory elements in Figure 1.4). Using a multicompartmental model of the VS cell network, Elyada et al. (2013) provided support that end inhibition increased the ratio of responses during rotation to responses during translation, thereby enhancing the relative sensitivity of the model to rotational flow fields. Hence, end inhibition, in addition to gap junction connections between neighboring LPTCs, appears to add to the rotational tuning of the VS-HS cell network.
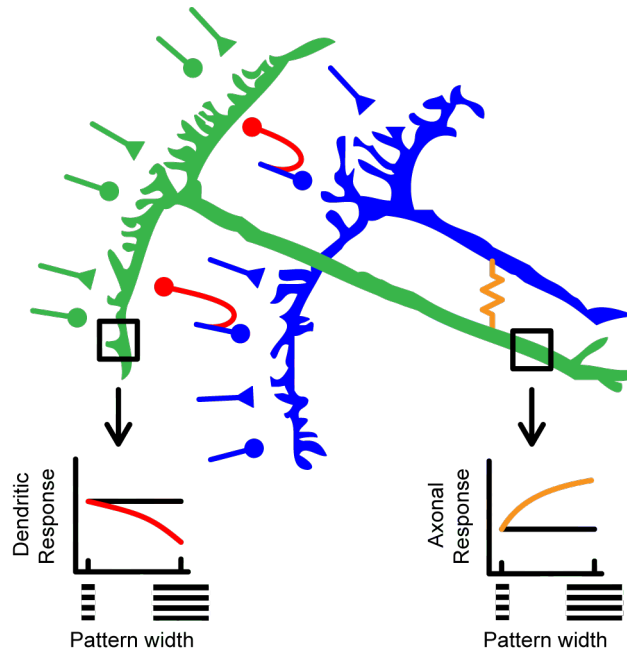
Figure 1.4: Schematic of end inhibition in a VS cell network. Two VS cells are shown in green (VS1) and blue (VS2). Direct excitatory (triangles) and inhibitory (circles) EMD inputs are depicted in the same color. In the absence of end inhibition, the expected response in the dendrites is independent of the width of moving patterns (left inset, black line). End inhibitory input to VS1 is shown as red collaterals, originating from direct inhibitory EMD input in the receptive field of VS2, as supported by the current injection experiments. This input decreases the response to wider patterns (left inset, red line). In the axon, the expected response is independent of pattern width (right inset, black line). The inclusion of a gap junction between the axons of VS1 and VS2 (orange connection) results in increased responses to increasing pattern width (right inset, orange line). For simplicity, end inhibition in VS2 is not shown. From Weir and Suver (2013).

LPTCs are believed to encode self-rotation and translation, and underlie stabilization reflexes of both the neck motor and wing motor systems during flight (Borst and Haag, 2002; Geiger and Nassel, 1981; Huston and Krapp, 2009; Krapp and Hengstenberg, 1996). Roll around different body axes produces characteristic flow fields, and Krapp and Hengstenberg (1996) showed that the ten VS cells in *Calliphora* are each tuned to motion that corresponds closely to rotational optic flow about different body axes. Based on this evidence, Krapp and Hengstenberg (1996) speculated that the ten VS cells are divided into three functional groups corresponding to roll, pitch,

and yaw[2]. In addition, it was proposed that these cells act as matched filters to detect particular types of optic flow fields (Franz and Krapp, 2000; Krapp et al., 1998). Although VS and HS cells have for the most part been described as rotation detectors, two studies, Kern et al. (2005) and Karmeier et al. (2006), provided evidence that they encode information about translational optic flow as well. Karmeier et al. (2006) showed that all six cardinal axes of self-motion (pitch, roll, yaw, up/down translation, sideways translation, and forward translation) can be encoded by combining the signals from different sets of VS and HS cells. Thus, the population of VS and HS cells, which are the main output neurons of the lobula plate, can, as a group, encode behaviorally relevant information about self-motion.

In addition to visual motion sensed by the compound eyes, it appears that VS cells may also receive input from the ocelli via the ocellar L-neurons. The anatomical evidence for L-neuron input to LPTCs is weak (Strausfeld, 1976), however Parsons et al. (2010) provided electrophysiological evidence that VS cells, which are tuned to rotation about 9 axes in *Calliphora* (Krapp et al., 1998), respond to ocellar stimulation, through which three axes of rotation are encoded. Although Parsons et al. (2010) do not mention the possibility, it seems feasible that the VS cells receive this ocellar input indirectly, via electrical connections with downstream neurons, for example. Thus the L-neurons may offer a rapid, low spatial resolution rotation signal together with the somewhat slower, high-spatial resolution measure of rotation from VS cells via the compound eyes, integrated by downstream neurons. Together, the ocellar and compound eye systems may provide a balance of speed and spatial resolution in the encoding of rotation by VS cells.

Self-motion information gleaned by the LPTC network is thought to contribute to stability during walking and flight. One of the established functions of the VS-HS network output is in mediating compensatory head movements to stabilize the retinal image. Flies control movement of the head using 21 neck muscles, each of which is typically innervated by a single motor neuron (Milde et al., 1987; Strausfeld and

---

[2]This concept was proposed earlier by Blondeau and Heisenberg (1982) based on behavioral studies using a *Drosophila* mutant with reduced optomotor responses.
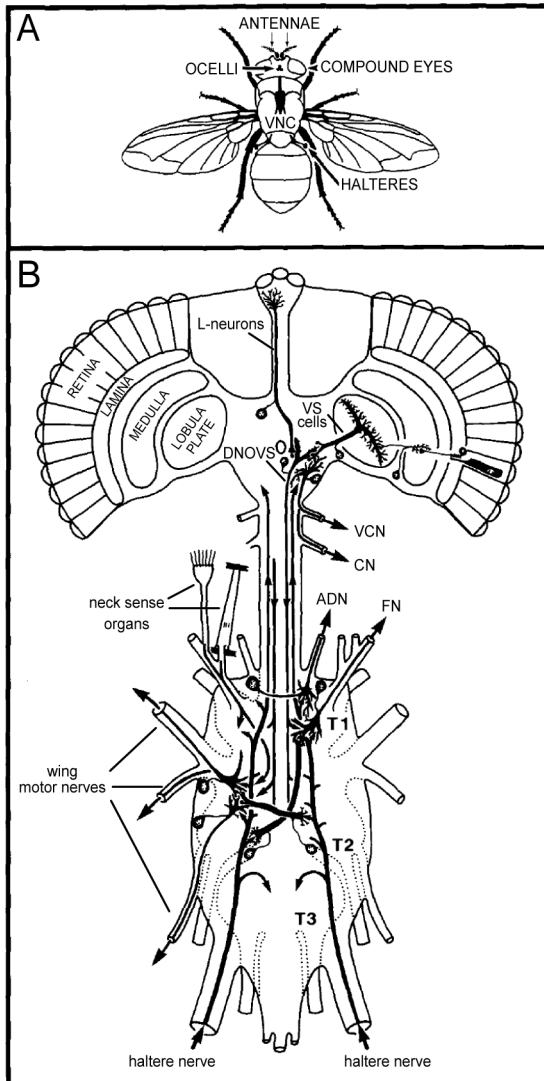
Figure 1.5: Visual input to the neck and wing motor systems. (A) Sensory structures that provide input to the neck and wing motor systems, shown in a dorsal view of a *Calliphorid* fly. Visual information from the ocelli and compound eye, along with mechanosensory information from the halteres and antennae, is relayed to neck motor neurons and to descending neurons that project to the ventral nerve cord (VNC). (B) Diagram of the brain and VNC (which consists of the three fused thoracic [T1-T3] and abdominal ganglia), showing the major visual neuropil, output elements of the visual system, and other nerves associated with the neck and wing motor systems. Lobula plate tangential neurons, such as VS cells, along with ocellar interneurons (L-neurons), send projections to the posterior slope where neck motor neurons and descending neurons (such as the DNOVS cells) receive input. The four major neck nerves are shown (VCN, CN, ADN, and FN). The haltere afferents and neck sense organs, which detect movements of the head, are also indicated. Additional inputs believed to be involved, including the Johnston's organ in the antenna and central neurons, are not shown. Modified from Hengstenberg (1991).

Seyan, 1985; Strausfeld et al., 1987). The neck motor neurons integrate information from ocellar interneurons, halteres[3], the wind-sensitive Johnston's organ on the antennae, and the LPTCs (Strausfeld and Seyan, 1985; Haag et al., 2010; Huston and Krapp, 2009) to stabilize gaze during walking and flying (Hengstenberg, 1991). Some neck motor neurons combine ocellar and LPTC input from both eyes (Huston and

---

[3]Halteres are small club-like appendages derived from the hindwings in true flies. The order name for flies, *Diptera*, meaning 'two wings' in Greek, reflects this. The halteres beat at the same frequency but anti-phase to the wings. They are necessary for stable flight, and haltere afferents detect Coriolis forces (Fox and Daniel, 2008; Pringle, 1948; Nalbach, 1993). These afferents provide rapid feedback to wing and neck motor neurons (Hengstenberg, 1991; Fayyazuddin and Dickinson, 1996).

Krapp, 2008; Wertz et al., 2012) and respond very closely to rotational flow fields, whereas others appear to respond to both translational and rotational motion (Huston and Krapp, 2008). In addition, the halteres gate the response of a number of neck motor neurons, and Huston and Krapp (2009) suggested that this fusion of haltere signals with LPTC output may contribute to fast head movements. Thus, self-motion information is encoded by the integration of visual motion information from LPTCs as well as other sensory modalities to control gaze. Figure 1.5 gives an overview of this anatomy. Furthermore, an unidentified central neuron, depending on behavioral state, may also provide input to neck motor neurons (Haag et al., 2010). How the LPTCs contribute to the control of the whole animal while navigating, via neck motor neurons or other descending cells, however, is not fully understood.

A few studies have attempted to directly address the influence of LPTCs on behavior. For example, Heisenberg et al. (1978) took advantage of a mutant fly, *optomotor-blind^{H31}*, that displayed deficits in optomotor turning responses, to try to answer this. VS and HS cells were absent in these flies. In walking *optomotor-blind^{H31}* flies, turning reactions were significantly reduced, but thrust and visually-induced landing responses were not. Based on observations from previous studies, Heisenberg et al. (1978) concluded that HS cells mediate turning responses, and that VS cells do not mediate thrust responses. The weaknesses in this study, however (admitted by the authors), is that the extent of this mutation is not well characterized. In a later study, Geiger and Nassel (1981) attempted to more precisely excise VS and HS cell function by ablating VS and HS neuron precursors on one side of the brain in third instar *Musca domestica* larvae. After each experiment, Geiger and Nassel (1981) examined the histology of the affected side to confirm the absence of VS and HS cells. This ablation protocol resulted in the absence of VS and HS cells with few other differences with the control (non-ablated) side of the brain, although the lobula plate of the ablated side was smaller in size. The authors claimed that the flies' optomotor responses to moving bars were not affected by the ablation, although the data presented in support of this is not entirely convincing given the large response variance (the authors claimed the difference lay within the standard deviation of the torque response, but

the responses appear very qualitatively different). Optomotor responses were affected by ablation of VS and HS cells, according to the authors, in an experiment in which a moving grating was presented instead of the stripe. The data for this experiment was not included in the publication, however, and so we are left to trust the word of the authors. In another experiment, Hausen and Wehrhahn (1983) microsurgically lesioned HS cell axons in *Calliphora erythrocephala* and observed a deficit in the torque response component associated with the lesioned right eye. These authors admitted that the lesion may not have been constrained to the HS cells only - such that downstream neurons receiving input from the HS cells may also have been damaged. In addition, it seems likely that output from other visual interneurons may also have been severed by the manipulation. Although this study showed a convincing deficit in turning responses induced by lesioning axons from one optic lobe, it is not clear that this can be attributed to HS cells alone. A similar, subsequent study by Hausen and Wehrhahn (1990) provided further evidence that severing LPTC axons reduces optomotor behavior. None of these studies provides a complete picture of the individual contribution of VS, HS, or other LPTCs in behavior, but they collectively support the view that lobula plate interneurons are involved somehow in mediating turning responses. It is important to remember in any functional study of the LPTCs that they are a network of neurons whose outputs are integrated by downstream neurons to extract behaviorally relevant information about self-motion. Indeed, the function of the LPTC neurons may be appreciated not just by direct ablation experiments, but by investigation of their output elements, which consist of the neck motor neurons already discussed, as well as descending interneurons that project to the ventral nerve cord.

A number of descending interneurons post-synaptic to the lobula plate have been characterized anatomically, although few electrophysiological studies exist. Most LPTCs project to the posterior slope (also called the lateral deuterocerebral neuropil; Strausfeld and Bassemir, 1985; Ito et al., 1998, see Figure 1.1), or further in towards the subesophageal ganglion (as HS cells do), where they make synaptic connections with descending neurons that project to neck, leg, and wing motor centers

in the thoracic ganglion (Strausfeld and Seyan, 1985; Strausfeld and Bassemir, 1985; Gronenberg and Strausfeld, 1990, see also Figure 1.5). A class of four descending neurons, called either 'descending neurons of the ocellar and vertical systems' (DNOVS, Strausfeld and Bassemir (1985)) or 'descending neurons of dorsal cluster 1' (DNDC1-1 to 1-4, Gronenberg and Strausfeld (1990)), receive input from VS cells and ocellar interneurons (Strausfeld et al., 1984). They respond to wide-field motion, antennal air currents, and momentary light intensity changes (Gronenberg and Strausfeld, 1990; Haag et al., 2007; Wertz et al., 2008), but their behavioral role remains uninvestigated. Yet recent technological advances in electrophysiology and quantitative analysis of behaving *Drosophila* have recently made it possible to investigate the function of this network in closer detail.

1.2 Electrophysiology in the behaving fly

A neural network cannot be fully understood by a connectivity map alone. Functional connectivity, which describes the activity pattern of a neural network, must be included in a comprehensive description of a neural network (Getting, 1989). Direct synaptic input can change the function of a neuron, but there are many other mechanisms that can affect the activity of a neuron, sometimes over long time scales, including neuromodulation and adaptation. These may only appear when a system is in a particular state, however, so methods that allow the observer to study a system in various states can help build the most complete picture of the function of a network.

The wealth of knowledge about LPTCs (Borst and Haag, 2002), the power of *Drosophila* as a model organism (Venken et al., 2011), and the amenability of fruit flies for quantitative behavioral analysis make this an extremely appealing system in which to study behavioral modulation of sensory systems. Until recently, electrophysiological recordings in behaving flies were not possible, so the LPTC network had been characterized solely in quiescent animals. However, recent studies have pioneered electrophysiological recordings in behaving *Drosophila* (Maimon et al., 2010; Chiappe et al., 2010), enabling researchers to measure VS and HS cell responses during flight

and walking, respectively, for the first time.

Using the preparation developed by Maimon et al. (2010), I was able to measure neural activity in a tethered, flying fruit fly (Figure 1.6). The fly is briefly anesthetized by chilling to approximately 4°C and glued (with UV-curing glue) to a custom-made Delrin holder. Through the top of this holder, I can access the brain for whole-cell patch clamp recordings or image neural activity using calcium indicators and two-photon microscopy. This holder design permits unobstructed movement of the fly's legs and wings, and flies in this preparation fly readily - I have observed flight bouts that last nearly an hour during a recording. Wild-type flies at near-room temperature rarely initiate flight spontaneously, but a small puff of air can be delivered towards the head to elicit flight. Flies are illuminated from behind by two fiber optics coupled to infrared LEDs at a wavelength not detectable by the fly visual system (880nm). I record behavior either with an infrared sensor whose signal corresponds to light intensity changes induced by movement of the wings. Despite some movement of the brain (presumably caused by the frontal pulsatile organ and/or other muscles in the head), recordings are typically stable for an hour or more. I control the temperature of the saline at all times using a perfusion input directed towards the exposed neuropil.

Maimon et al. (2010) used this physiology preparation to reveal a number of physiological changes that occur in VS cells during flight, two of which are particularly salient. At the onset of flight, the baseline membrane potential of the VS cells as measured at the cell body rapidly shifts upward, and the amplitude of the responses to large field visual motion increases (Figure 1.7). Whereas the baseline membrane potential remains elevated during flight and returns to the pre-flight potential rapidly at the end of a flight, the gain boost in visual response decays slowly during a long flight bout and returns to baseline after flight over a 20 s period (Figure 6C, Maimon et al. (2010)). The different time course of the baseline shift and gain boost suggests that different underlying mechanisms are at work, with the slower dynamics of the gain boost suggestive of the action of neuromodulators (Marder and Calabrese, 1996; Burrows, 1996; Siegelbaum and Tsien, 1983). In another recent study, Chiappe et al. (2010) showed, using calcium imaging, that HS cells increase in gain during walking,
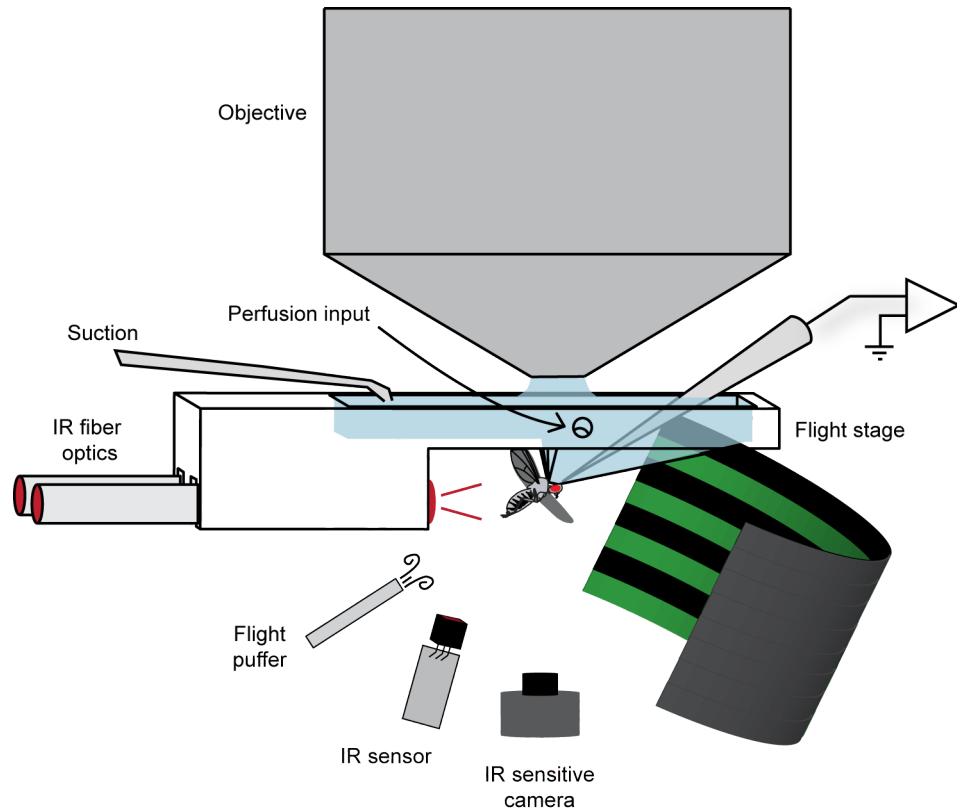
Figure 1.6: Schematic of the physiology/imaging preparation (electrode not present during imaging). Not all components are drawn to scale.

consistent with effects observed in VS cells. These studies demonstrate that the responses of LPTCs, long characterized only in quiescent animals, are subject to modulation during different behaviors.

1.3 Neuromodulation in insect sensory systems

The profound influence of chemical modulators on neural circuits gained appreciation in the 1980's, when it became clear that a connectivity diagram alone was not sufficient to understand neural circuits (Getting, 1989; Bicker et al., 1989). Today, we know that neuromodulators can act at every level of a neural circuit, from sensors to muscles, and can fundamentally alter the output of a given circuit (Marder, 2012). The term 'neuromodulator' may refer to any chemical released by a neuron that alters the function of a neuron or often a group of neurons (Burrows, 1996),
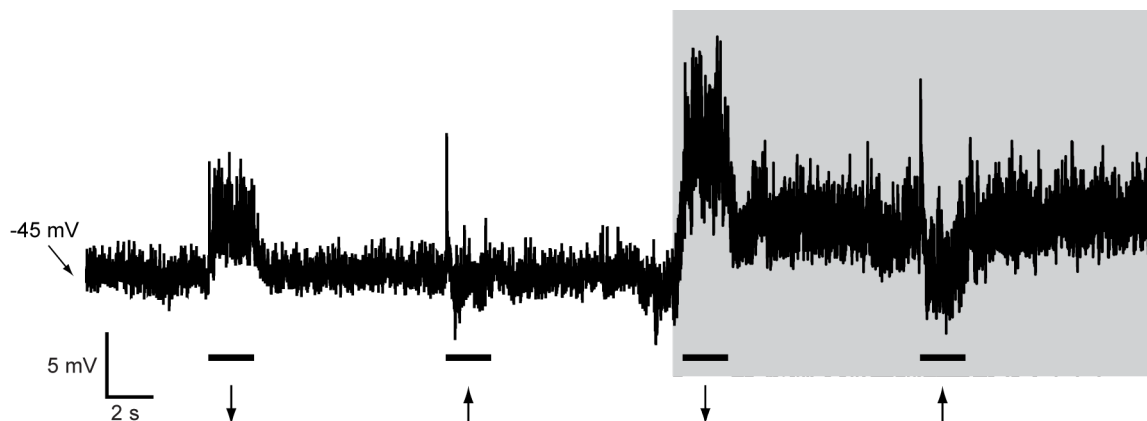
Figure 1.7: Flight effects in VS cells. Example trace showing flight effects in one VS cell. Membrane potential response of a VS3 cell to 2 s trials of a sine wave grating moving downward at 1 Hz (a stationary mean luminance pattern was presented between motion trials). The grey shaded region indicates when the fly was flying. Black bars indicate when stimulus was in motion. Baseline membrane potential is indicated by the black arrow. Only the responses at the start of this flight are shown for clarity (this flight bout lasted a total of 4.6 minutes).

and includes transmitters such as GABA, acetylcholine, glutamate, biogenic amines (e.g. dopamine, serotonin, and octopamine), and peptides. Most often, neuromodulators bind to G-protein coupled (or metabotropic) receptors, but examples of neuromodulators directly gating of ion channels also exist (Taghert and Nitabach, 2012). Invertebrate systems have proved particularly fruitful for studying neuromodulation (Marder and Bucher, 2007; Bargmann, 2012; Taghert and Nitabach, 2012; Kravitz and Huber, 2003), and powerful new tools developed in model organisms may allow us to investigate the mechanisms of this modulation in even greater detail (Bargmann, 2012; Inagaki et al., 2012).

The increased gain in visual interneurons described in Section 1.2 is reminiscent of neuromodulator action based on its dynamics, and I hypothesized that the neuromodulator octopamine might be involved in producing this change. Octopamine (Figure 1.8), whose prefix 'oct' comes not from its chemical structure, but from its discovery in the salivary glands of octopuses (Erspamer, 1948), is a member of the group of biogenic amines that includes dopamine, and is thought to be the chemical analog of norepinephrine in vertebrates. Nearly every physiological process in

invertebrates involves octopamine (Roeder, 1999), and it is thought to play a role in coordinating aspects of many behaviors including learning and memory (Menzel and Muller, 1996; Schwaerzel et al., 2003; Davis, 2005), aggression (Kravitz and Huber, 2003; Zhou et al., 2008; Hoyer et al., 2008), egg-laying (Monastirioti et al., 1996), and flight (Orchard et al., 1993; Adamo et al., 1995). Octopamine's role in regulating physiology during flight has been particularly well characterized in the locust.
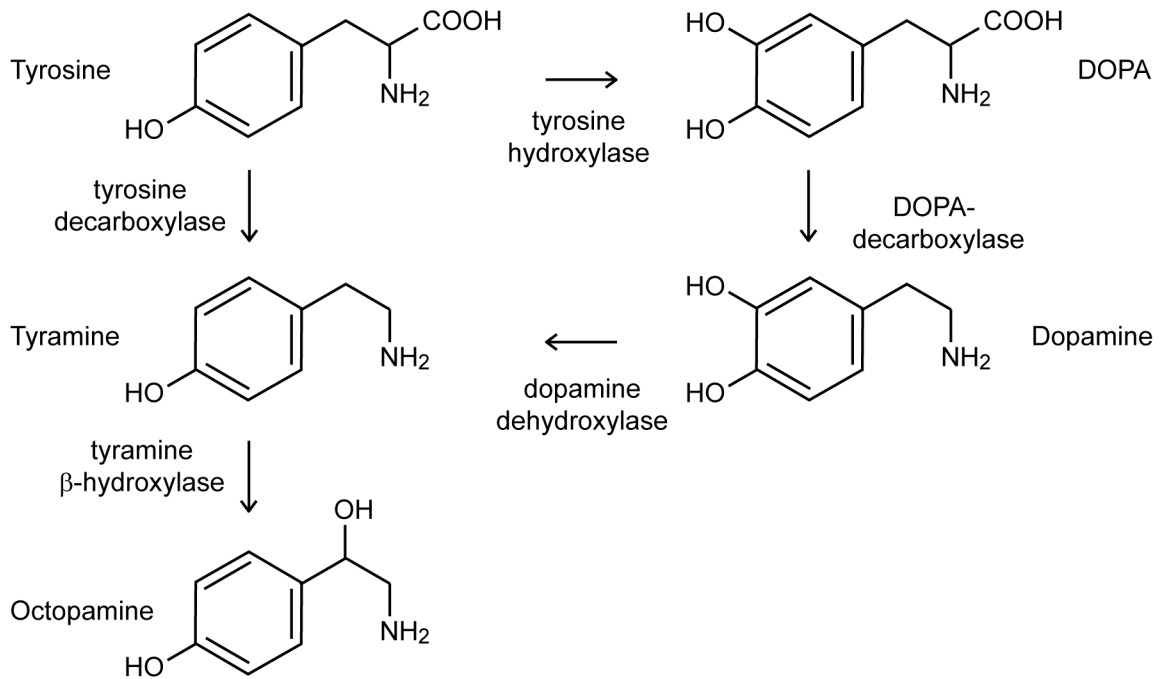
Figure 1.8: Octopamine synthesis pathway. Octopamine is a member of the family of biogenic amines that includes dopamine. Octopamine is synthesized from tyramine by the enzyme tyramine ß-hydroxylase. Tyrosine, the precursor to tyramine, is synthesized by the enzyme tyrosine decarboxylase 2 (Tdc2) in neurons, or by tyrosine decarboxylase 1 (Tdc1) in other tissues .

1.3.1 The role of octopamine in locust flight and escape behavior

A large body of research from locusts suggests octopamine orchestrates physiological changes throughout the body during flight. The formal 'octopamine orchestration' hypothesis, first proposed by Sombati and Hoyle (1984), speculated that specific sets of octopaminergic neurons were involved in generating specific behaviors. Consistent

with this hypothesis, certain octopaminergic cells in the locust brain, such as the dorsal unpaired median (DUM) neuron, become tonically active during flight (Ramirez and Orchard, 1990). Furthermore, pharmacological application of octopamine appears to elicit a general arousal process influencing many features of the animal's flight system including proprioceptors, interneurons, and muscles (Orchard et al., 1993). With respect to possible effects on visual processing, there is a set of seven octopaminergic neurons in the locust brain with extensive arborizations in the optic lobes, and two of these may play a role in dishabituation of the visual system (Stern et al., 1995). For example, the octopaminergic PM4 neuron, which responds to visual, wind, and tactile stimuli, innervates a large region of the optic lobes, and is thought to dishabituate lobula giant motion detector (LGMD) via endogenous release of octopamine (Roeder, 1999; Stern et al., 1995). The LGMD then projects to the descending contralateral movement detector (DCMD), a multimodal descending interneuron involved in escape reflexes (Bacon et al., 1995; Rowell, 1971; Pearson et al., 1980; Fotowat et al., 2011). Thus, octopamine appears to play a role in visually mediated behaviors in the locust.

1.3.2   Modulation of visual interneurons in flies

More recently, studies in blowflies have shown that the octopamine agonist chlordimeform can modulate the response properties of lobula plate tangential neurons in a manner similar to that observed in flight (Jung et al., 2011; Longden and Krapp, 2009, 2010). Specifically, chlordimeform, when bath-applied, induced an increase in response range and decreased latency of two spiking LPTCs, V1 and V2 (Longden and Krapp, 2009). Similarly, chlordimeform induced an increase in spontaneous activity, a frequency-dependent decrease in motion adaptation, and an increased response gain to moving gratings in the horizontally sensitive H2 neuron. Furthermore, Jung et al. (2011) showed that during flight, the response of H1 increases at higher temporal frequencies, and that chlordimeform roughly reproduced this increase. Recently Rien et al. (2012) also found evidence that chlordimeform reduces the contrast

gain adaptation of V1 and H1 neurons, and hypothesized that this adaptation occurs presynaptic to the LPTCs. Together, these studies showed that the activity of LPTCs is altered by the octopamine agonist chlordimeform, and suggest that flight may alter their response properties via octopamine. However, these results left unclear what the neuronal basis of such modulation might be, and what functional effect this may have for the behavior of the animal.

1.4   Thesis overview

In this thesis, I describe a body of work aimed at determining the mechanism and function of the flight effects observed in the visual system of *Drosophila melanogaster*. I begin by characterizing the neuronal basis of the flight effects observed in visual interneurons and provide strong evidence that octopamine neurons that project to the optic lobe become active during flight, and are necessary and sufficient to produce the flight boost in VS cells. In the hopes of determining the role of single octopamine neurons in this system, I then use intersectional genetic tools to manipulate the activity of a single octopamine neuron that projects to many regions of the optic lobes, including the lobula plate, where the dendrites of the behaviorally modulated visual interneurons are located. I also explore the origin of the flight boost by quantifying the effect of wind stimuli on responses of VS cells. Lastly, we examine the functional consequences of the flight changes by manipulating the activity of octopamine neurons in freely flying flies, and provide preliminary evidence that these neurons underlie a gain mechanism that underlies flight speed control.

Chapter 2

Octopamine neurons mediate flight-induced modulation of visual interneurons in *Drosophila*

2.1 Introduction

Recent studies showed that the activity of VS cells is modulated during flight (Maimon et al., 2010), and pharmacological experiments in blowflies (see Section 1.3.2), as well as a wealth of evidence in locusts (Section 1.3.1), suggest that parts of the insect visual system may be modulated by octopamine. However, the role of octopamine in modulating these effects in behaving *Drosophila* was not established. We used a combination of whole cell patch clamp recordings and calcium imaging in tethered, flying *Drosophila* to assess whether or not octopamine neurons play a definitive role in modulating VS cells. To more fully characterize the responses of VS cells in both quiescent and flying flies, I first quantified the average responses to large field vertical motion across a range of temporal frequencies. I then measured the effect of exogenous application of octopamine, which produced similar effects in VS cells as observed during flight. Next, using the genetically-encoded calcium indicator GCaMP3 (Tian et al., 2009) we tested whether octopamine neurons become active during flight. Finally, I manipulated endogenous release of octopamine through ectopic expression of dTrpA1 and Kir2.1 channels and was able to reproduce or abolish aspects of the naturally occurring flight boost. These results provide the first evidence that octopamine cells

increase in activity during flight in *Drosophila*, and are both necessary and sufficient to produce the flight boost in VS cells.

2.2   Experimental procedures

2.2.1   Animals

I used 1-3 day old female *Drosophila melanogaster* raised on standard cornmeal medium at 25°C with a 14:10 light/dark schedule. Our experiments made use of the following transgenic constructs: *DB331-Gal4* (Scott et al., 2002, FBti0115113), *UAS-2xEGFP* (Bloomington 6874), *Tdc2-Gal4* (Bloomington 9313), *UAS-red stinger* (FBtp0018199), *UAS-mCD8GFP* (FBst0005137), *UAS-GCaMP3* (Tian et al., 2009), *UAS-dTrpA1* (Bloomington 26263), and *UAS-Kir2.1-EGFP* (FBti0017552). For some fly strains, we crossed in the *white* (*w+*) gene onto the first chromosome (using the Heisenberg Canton-S background) so that all flies had one functioning wild-type copy of the gene. See Table 2.1 for complete genotypes of these flies. To encourage long flight bouts, I removed the pro- and meso-thoracic legs.

2.2.2   Whole cell patch clamp recordings

Using a preparation described previously (Maimon et al., 2010), I performed whole-cell patch clamp recordings on VS cells 1-4 in the right brain hemisphere (Figure 1.6). In some experiments, I used EGFP to target VS cell bodies by using *DB331-Gal4*, *UAS-2xEGFP* flies with subsequent verification of cell identity using dye fills (see Figure 1.2) as well as the electrophysiological responses. For all other experiments in which the VS cells were not labeled with EGFP, I identified the cell type after each experiment using dye fills and cell response properties alone.

I used electrodes with resistances of 4.8-7.4 MΩ. Our intracellular, external, and collagenase solutions were identical to those used in Maimon et al. (2010). I added 20μM Alexa 568 (Invitrogen #A-10437) and 13mM biocytin (Invitrogen #B1093) to the intracellular solution for cell visualization. For 13 cells, I omitted biocytin and

Name	Chapter	Full genotype	Bloomington #	Flybase #	Notes & references
DB331-Gal4	2, 4	*w+, DB331-Gal4; +; +*	N/A	FBti0115113	Scott et al. (2002). Crossed out *w[*]*. Not publicly available.
UAS-2xEGFP	2, 4	*w[*]; P{w[+mC]=UAS-2xEGFP}AH2; +*	6874	FBst0006874	
Tdc2-Gal4	2	*+ (HCS); P{w[+mC]=Tdc2-GAL4.C}2; +*	9313	FBst0009313	Crossed out *w[*]*
UAS-GCaMP3	2	*+ [HCS]; pJFRC-MUH{UAS-GCaMP3.0}attP40; +*	32116	FBti0131642	Tian et al. (2009). Crossed out *w[*]*
UAS-dTrpA1	2	*w[*]; P{w[+mC]=UAS-TrpA1.K}attP16; +*	26263	FBst0026263	
UAS-Kir2.1	2	*w[*]; +; P{w[+mC]=UAS-Hsap\KCNJ2.EGFP}7*	6595	FBti0017552	Experimental flies
UAS-Kir2.1	2	*+ (HCS)/w[*]; +; +/P{w[+mC]=UAS-Hsap\KCNJ2.EGFP}7*	6595	FBti0017552	Control flies. Crossed out *w[*]*

Table 2.1: Transgenic lines.

observed no obvious effect in the physiological responses. The average resting potential of cells after compensation for an experimentally-measured junction potential (-13mV) was -46.4mV. I injected 20-30pA constant hyperpolarizing current into the cells prior to presentation of visual stimuli to aid with dye fills, which decreased the membrane potential by an average of 3.6mV (to -50.0 mV). The access resistance (R_{acc}) for all recordings was 31.8 +/- 6.8 MΩ S.D., which is in the typical range for *Drosophila* whole-cell patch clamp recordings (Wilson et al., 2004). Any cells with R_{acc} greater than 50MΩ were excluded from my analysis.

I controlled the temperature of the bath with a bipolar temperature controller and an in-line heater/cooler (CL-100 and SC-20, Warner Instruments). For all experiments, with the exception of dTrpA1-activation and parental controls, I raised the bath temperature to 30°C during the initial desheathing step, and then lowered the bath to temperature 19°C for the remainder of the experiment. I performed the desheathing without any applied heat in all dTrpA1 activation and parental control experiments to avoid contaminating results with pre-exposure to heat. For these dTrpA1 activation experiments, I held the external saline at 19°C, increased it to 28°C over a time course of approximately 120 s, and then lowered it back to 19°C.

2.2.3 Visual display and stimuli

I presented flies with vertically-moving sine wave grating stimuli (8 pixels, approximately 20° per cycle) using an electronic LED display (Reiser and Dickinson, 2008) as described in Maimon et al. (2010). I presented upward and downward-moving stimuli at a temporal frequency of 1, 2, 4, 8, 16, or 24 Hz, as well as a stationary sine wave grating (0 Hz), in pseudorandom order. In addition, I presented the visual stimulus beginning at a position chosen randomly from one of four quadrants in the sine-wave pattern. VS cells showed a slight decay in response over multiple cycles of this stimulus, so I presented each stimulus for 1 to 4 s to obtain a measure of at least four cycles. Thus, I presented 0, 1, 2, 4, 8, 16, and 24 Hz stimuli for 1, 4, 2, 1, 1, 1, and 1 s, respectively. I presented 1 s of stationary mean luminance between stimuli.

2.2.4 Pharmacology

I dissolved octopamine (DL-Octopamine hydrochloride, Fluka) in extracellular saline at a concentration of 100μM on the day of each experiment. For comparison, this concentration of octopamine, the lowest level at which VS cell responses were noticeably and reliably affected, lies at or near concentrations used in previous studies in locusts (Ramirez and Pearson, 1991; Matheson, 1997), crustaceans (Goaillard et al., 2004), and crickets (Kosakai et al., 2008). To my knowledge, no measurements have been made of in vivo concentrations of octopamine in various tissues in the brain of *Drosophila* for comparison. Octopamine levels in the hemolymph of crickets (Adamo et al., 1995) and locusts (Goosey and Candy, 1980) become elevated during flight (235.5+-117.7 nM and 173+-8nM , relatively), and although the levels used in previous pharmacology experiments surpassed these concentrations, it is unclear how hemolymph levels correlate with that of the neuropil where neurons of interest are located. I modified the holder from Maimon et al. (2010) to more rapidly apply octopamine by aiming the perfusion input directly towards the exposed neuropil. The cells never fully recovered to pre-octopamine levels of activity during a washout of octopamine, so I do not present these responses.

2.2.5 Immunohistochemistry

We dissected brains in 4% paraformaldehyde in PBS and fixed for a total of 30 minutes. We then incubated them overnight at 4°C in a primary antibody solution containing 5% normal goat serum in PBS-Tx, mouse anti-nc82 (1:10, DSHB) and rabbit anti-GFP (1:1000, Invitrogen). Brains were then incubated overnight at 4°C in a secondary antibody solution containing 5% normal goat serum in PBS-Tx, goat anti-mouse Alexa Fluor 633 (1:250, Invitrogen) and goat anti-rabbit Alexa Fluor 488 (1:250, Invitrogen). We then mounted the brains in Vectashield and imaged them on a Leica SP5 II confocal microscope under 40x magnification and scanned at 1μm section intervals. We adjusted intensity and contrast for single channels for the entire image using ImageJ 1.45s.

2.2.6   Calcium imaging

Using the same holder and procedures as in the electrophysiology experiments, we[1] tethered flies to the holder and removed the cuticle and fat tissue above either the lobula plate or the posterior slope surrounding the esophagus foramen to gain optical access to putative dendrites of octopamine neurons that project to the optic lobes (Busch et al., 2009).

We imaged the brain using the Prairie Ultima IV two-photon excitation microscope controlled by Prairie View Acquisition software (Prairie Technologies). We used a mode locked Ti:Sapphire laser (Chameleon Ultra; Coherent) tuned to 930 nm as an excitation light source and adjusted the laser power to be 20 mW at the rear aperture of the objective lens (Nikon NIR Ap, 40x water-immersion lens, 0.8 NA). We collected fluorescence using a multi-alkali photomultiplier tube (Hamamatsu) after bandpass filtering it with an HQ525/70m-2p emission filter (Chroma Technologies). We acquired images in a frame scan mode (152x150 pixels, 0.125 s/frame) to record activity of octopamine neurons. For each trial, we acquired images for 30 s, starting from 10 s before the flight onset. For each fly, we acquired a z-stack image (z step = 1 µm) covering the entire dendritic branch of the octopamine neurons near the esophagus foramen to confirm the location of each recording within the brain.

2.2.7   Data analysis and statistics

For whole cell patch clamp recordings, I acquired data at 10 kHz using Axoscope software. All data analyses were done using Matlab R2010b. I calculated peak visual responses by first down-sampling the data to 1 kHz. I then calculated a moving average of the membrane potential over a window of 10 points (10 ms) and selected the peak during the first cycle of stimulus motion.

To initiate flight, I applied a small puff of air directed towards the fly's head. If flight was not initiated after a puff, I observed an increase in visual responses that

---

[1]Akira Mamiya performed the calcium imaging experiments described in this chapter. Any use of the first person plural in this chapter and subsequent chapters, when discussing the calcium imaging experiments, should be interpreted to include him.

returned to pre-puff levels in 20 s or less. Thus, I excluded visual responses from the measure of quiescent responses for 20 s after I applied a puff of air if the fly did not initiate flight. This resulted in at most a difference of -0.27 mV in average quiescent visual response. I used one- and two-tailed Student's t-tests to make statistical comparisons of the data.

For two-photon imaging experiments, we applied a brief puff of air to the head of the fly to initiate flight, as in the electrophysiology experiments. If a fly was still flying after the end of two-photon image acquisition (approximately 20 s after the onset of flight), we terminated the flight by manually delivering a second puff of air. We waited 4 minutes between initiations of flight in the same animal. Only flies that flew for at least five bouts lasting 12 s or more were included in the analysis. Throughout the experiment, we illuminated the fly from behind with a high-intensity infrared diode (880nm; Golden Dragon; Osram) and used a Basler A602f camera with a fixed-focus lens (Infinistix 90, 94 mm working distance, 1.0x magnification) to record the behavior of the fly from below at 100 frames/s. We used FView (Straw and Dickinson, 2009), an open source program written in Python, to record images of flies simultaneously with a signal that indicates the timing of two-photon image acquisition. We analyzed images using custom software written in Matlab 2011b. We identified the stereotypic cluster of thick dendritic branches of octopamine neurons and terminal regions in the lobula plate based on the basal fluorescence of GCaMP3 and chose this area as a region of interest (ROI). We then averaged the pixel intensity in the ROI to estimate the fluorescence from this region. We first smoothed the acquired images with a Gaussian filter (3 x 3 pixel, $\sigma = 0.5$) and corrected for small movements of the brain in the x-y direction during the image acquisition using a previously published algorithm (Guizar-Sicairos et al., 2008). We then averaged the pixel intensity in the ROI to estimate the fluorescence from this region. For each trial, we reviewed the images of flight behavior and determined the flight onset time by finding the first frame after the application of the air puff where a fly moves its wing forward. We then used the simultaneously recorded signal that indicates the timing of two-photon image acquisition to find the frame in the calcium imaging that corresponds to flight

onset time. We used average fluorescence during the five s period before the onset of the flight as baseline fluorescence (F0) and used this value to calculate the $\Delta F/F$ signal (defined as (F-F0)/F0). We calculated mean $\Delta F/F$ signal for each fly using 5 to 6 trials.

2.3   Results

2.3.1   Flight-dependent modulation of VS cell response amplitude depends on temporal frequency of motion

Previous results indicate that the physiological properties of VS cells are modulated during flight (Maimon et al., 2010). Before investigating the effects of octopamine in this system, I wished to characterize more completely the flight modulation observed in this earlier report. Specifically, flight-dependent observations in VS cells were quantified in Maimon et al. (2010) at a single temporal frequency (1 Hz), so it remained unclear how the flight boost might vary across the broad tuning curve of these cells (Joesch et al., 2008). As indicated in Figure 2.1, I presented flies with large field upward and downward motion across temporal frequencies ranging from 1 to 24 Hz (Figure 2.1C). The responses of VS cells during quiescence were strongest at a temporal frequency of 1 Hz and exhibited phase-locking with the motion stimulus, consistent with previous studies (Joesch et al., 2008). The responses to a stepwise change in motion at all temporal frequencies exhibited an early peak followed by a gradual decay, with the rate of decay tending to increase with increasing temporal frequency. Given these dynamics, I chose to further quantify and compare cell responses throughout the paper by measuring the baseline-subtracted peak response to downward visual motion, as indicated in Figure 2.1B, although analyses based on steady state responses and/or responses to upward motion lead to identical conclusions (data not shown). Our results are consistent with recent studies from walking *Drosophila* (Chiappe et al., 2010) and flying blowflies (Jung et al., 2011), which showed that these behaviors are associated with an increase in the visual responses of HS and H1

neurons at many temporal frequencies. As in these studies, I observed a broadening of the tuning curve at higher frequencies during locomotion. In contrast to the results of these prior studies, I did not observe an upward shift in the temporal frequency that elicits a maximal response in VS cells, nor do I observe as large an effect at the highest temporal frequencies. The results of our temporal frequency analysis indicate that the VS cell responses in both quiescent and flying preparations are greatest at a temporal frequency of 1 Hz, and that the flight-dependent boost in visual responses is actually greatest at temporal frequencies of 2 to 8 Hz (Figure 2.1D and 2.1E). This effect of flight represented a 20-30% increase in response as measured at the cell body of the VS cells.

2.3.2   Bath application of octopamine reproduces flight effects in quiescent flies

Given the wealth of evidence linking octopamine to flight modulation in insects (Brembs et al., 2007; Goosey and Candy, 1980; Longden and Krapp, 2009; Jung et al., 2011; Orchard et al., 1993; Ramirez and Orchard, 1990; Sombati and Hoyle, 1984), I hypothesized that octopamine might be responsible for these physiological changes during flight. I measured the responses of VS cells to visual motion across the same range of temporal frequencies used in the experiments described above before and during bath application of 100 µM octopamine. Upon octopamine application, the resting potential of the VS cells rose and their response to visual motion increased, similar to the effects observed during flight (Figure 2.2). Application of control saline did not induce either of these two effects (Figure 2.3). During octopamine application, baseline membrane potential shifted upward during flight by 2.24 +/- 1.2mV, which is smaller but not significantly different (at P = 0.05 level) than the baseline shift produced during flight in the absence of octopamine (3.42 +/- 1.5mV; two-tailed Student's t-test; P = 0.051; Figure 2.4). However, no additional increase in the visual response to motion was observed in the VS cells when the animals were flying. These results show that octopamine, when applied exogenously, can mimic the changes in
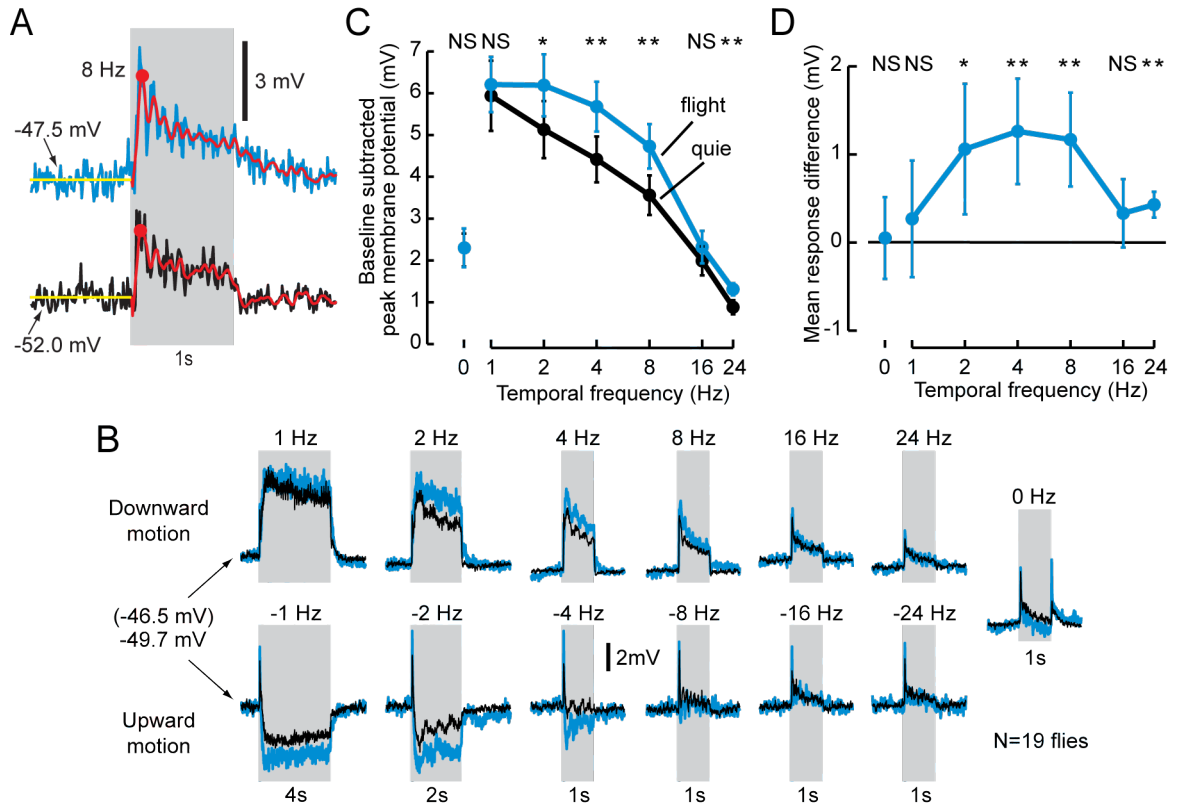
Figure 2.1: Flight boost varies across a range of temporal frequencies. (A) Example response of one VS cell to a downward-moving sine wave grating pattern at a temporal frequency of 8 Hz. Quiescent ('quie') response is shown in black and the response during flight in blue. The grey shaded region indicates when the visual stimulus was in motion. The peak response to motion is indicated by the red dot (obtained from the smoothed response during motion, see Methods), and the average baseline membrane potential during 1 s immediately before motion onset is indicated by the yellow line. (B) Average visual responses of 19 flies. Responses to downward motion (top row), upward motion (bottom row) and a stationary sine-wave grating (rightmost trace). The flight responses (blue traces) have been baseline subtracted relative to the quiescent baseline membrane potential (black traces). The average baseline membrane potential during quiescence is shown, along with the average baseline membrane potential during flight before baseline subtraction (in parentheses). Visual motion was presented for four or more cycles at each speed, so some traces have been condensed for space considerations. (C) Temporal frequency tuning curve for downward motion responses. Abscissa is plotted on a log scale. Points represent the mean response across 19 flies. The response for each fly was computed by subtracting the average membrane potential during the 1 s before motion (yellow line in A) from the peak membrane potential during the first cycle of motion (red dot in A). Lines indicate standard error about the mean. (D) Difference between flight and quiescent baseline-subtracted responses. Abscissa is plotted on a log scale. The average difference for each fly was computed separately and the mean and standard error across all flies is shown. In C and D asterisks indicate speeds at which the difference between flight and quiescent responses (computed for each fly) was significantly greater than zero (paired Student's t-test). Single and double asterisks indicate significance at alpha = 0.05 and 0.01, respectively. NS indicates no significance at alpha <= 0.05.

VS cell responses to motion observed during flight.

2.3.3 Octopaminergic neurons with optic lobe projections show an increase in activity during flight

Although octopamine application induces changes in VS cell physiology that resemble those observed in flight, pharmacology alone cannot prove the role of endogenous octopamine neurons in the flight boost. One critical prediction of this hypothesis is that octopamine neurons must become active at the onset of flight. A set of six octopaminergic neurons (called AL2 neurons by Busch et al., 2009 and G3a neurons by Sinakevitch and Strausfeld, 2006) send projections to the optic lobes, making them good candidate neurons for the modulation of visual responses. These neurons each send a large process along the esophageal foramen before reaching the posterior slope (Busch et al., 2009). Using a selective driver line (*Tdc2-Gal4*, Busch et al., 2009), I made an attempt to conduct whole cell patch recordings from octopamine neurons, however the position of the cells bodies within the brain prohibited the use of a gentle enough dissection to permit recordings in flying animals. As an alternative strategy, we used the same driver line to express the genetically-encoded calcium indicator GCaMP3 (Tian et al., 2009), and measured their calcium activity during flight using 2-photon imaging. Although the Gal4 driver line we used likely targets all octopamine neurons, we restricted our analysis to two areas, the lobula plate and the region of brain surrounding the esophageal foramen where the optic-lobe projecting cells have large and overlapping dendrites (Figure 2.4A). During flight, the activity of octopamine cells in these two regions increased (Figure 2.4B), suggesting that they could indeed serve a role in modulating the activity of neurons within the optic lobes during flight. The time course of the GCaMP3 signal was slightly different in the two regions, with the fluorescent change decaying more rapidly in the fine terminals of the lobula plate. Without simultaneous electrophysiological recordings or neurochemical measurements, we cannot determine how the GCaMP3 signal correlates with either firing rate or transmitter release. We verified that the response was not a motion
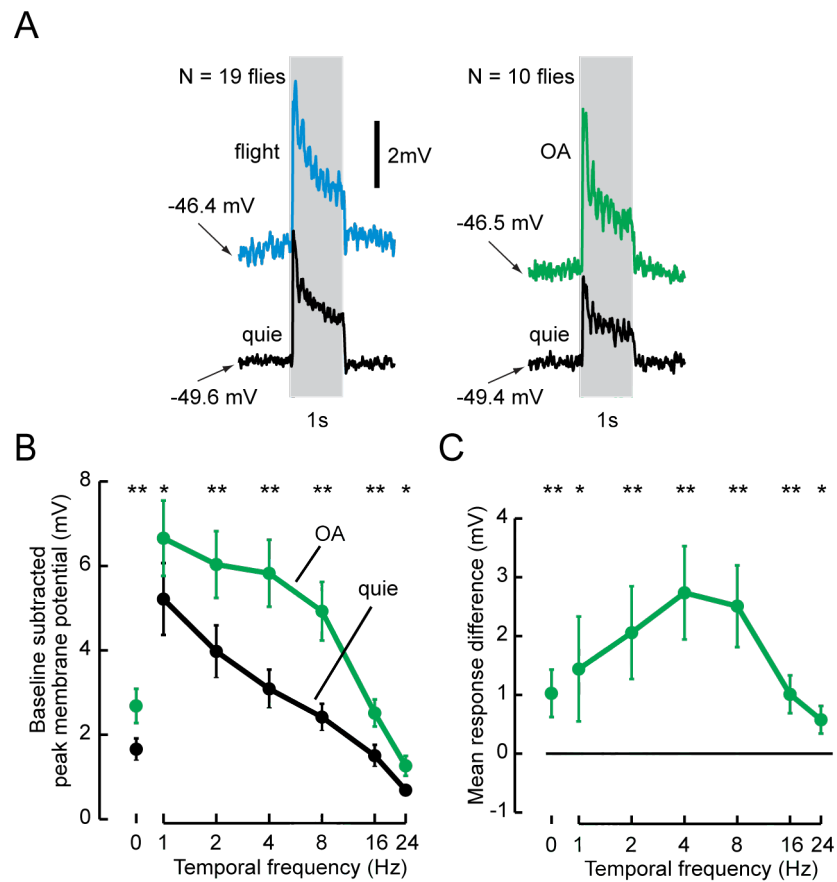
Figure 2.2: Octopamine reproduces flight effects. (A) Average visual response to 8 Hz downward motion during flight (left, blue trace) and during octopamine application (OA; right, green trace) and corresponding quiescent responses ('quie', black traces). The grey shaded region indicates when the visual stimulus was in motion. The average baseline membrane potential during the 1 s immediately before motion onset is shown for quiescence, flight and OA. (B) Temporal frequency tuning curve for downward motion responses during quiescence and octopamine application. Abscissa is plotted on a log scale. (C) Difference between motion responses during quiescence and octopamine application. Abscissa is plotted on a log scale. In B and C responses and statistics were computed as described in Figure 2.1D and 2.1E. Asterisks indicate speeds at which the difference between the responses during octopamine application and quiescence (computed for each fly) was significantly greater than zero (paired Student's t-test). Single and double asterisks indicate significance at alpha = 0.05 and 0.01, respectively.
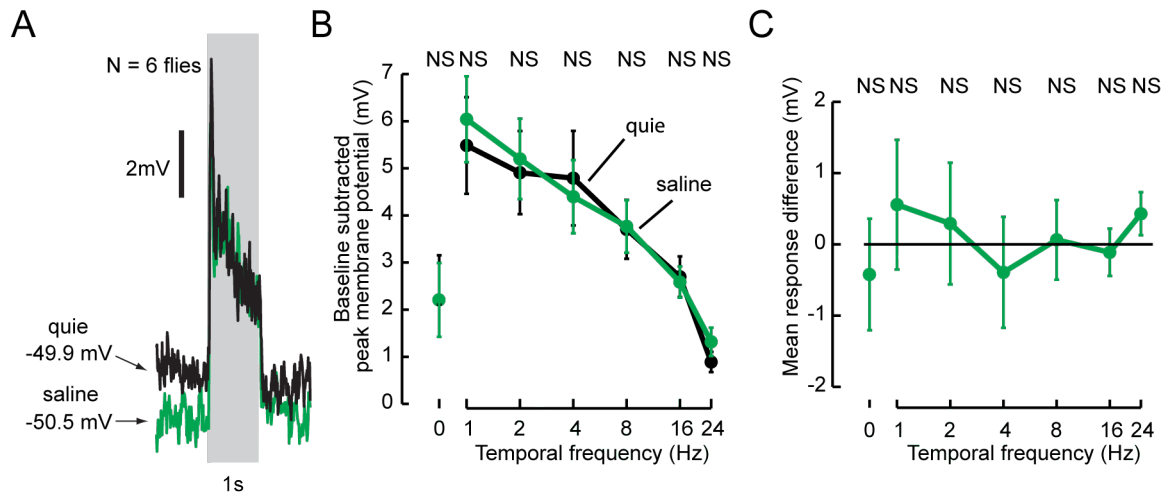
Figure 2.3: Saline control for octopamine pharmacology. (A) Average visual response to 8 Hz downward motion during saline application (green trace) and corresponding quiescent responses ('quie', black traces). The grey shaded region indicates when the visual stimulus was in motion. The average baseline membrane potential during the 1 s period immediately before motion onset is shown for quiescence and saline. (B) Temporal frequency tuning curve for downward motion responses during quiescence and saline application. Abscissa is plotted on a log scale. (C) Difference between motion responses during quiescence and saline application. Abscissa is plotted on a log scale. In B and C, NS indicates speeds at which the difference between saline and quiescent responses (computed for each fly) was not significantly greater than zero (paired Student's t-test, alpha = 0.05).

artifact by driving expression of EGFP instead of GCaMP3 in octopamine neurons, and observed no change in fluorescence in the overlapping dendrites during flight (Figure 2.4B).

2.3.4 Activation of octopamine neurons causes an increase in VS cell responses to motion

In the first sets of experiments in this chapter, we found that exogenously applied octopamine mimics the effects seen in VS cell responses during flight and that octopamine neurons that project to the optic lobes are active during flight. The two remaining critical tests are that activation of octopamine neurons are both sufficient and necessary to induce the physiological changes observed during flight. To test for sufficiency, I expressed dTrpA1 channels in octopamine neurons using the *Tdc2-Gal4* driver and tested whether I could reproduce the flight effect in quiescent flies by activating the octopamine neurons with temperature. In these experiments (and all subsequent experiments described in this paper) I did not co-express EGFP in VS cells for identifying the somata for recording. However, I was able to target VS cell bodies for recording based on their relative size and position in the brain, and could unambiguously identify the cells after each experiment using a combination of response properties and anatomy. Using a non-permissive temperature that matched our previous experiments (19°C), I first measured the pre-heat responses of VS cells across the range of temporal frequencies. I then quickly (within 120 s) clamped the temperature of the external saline to 28°C in order to activate dTrpA1 channels, and measured the responses of the VS cells. Many flies responded to the elevation of bath temperature by spontaneously initiating flight, but in these cases I waited until they stopped flying before beginning our measurements of VS cell responses. I also lowered the temperature back to 19°C to record post-heat responses. Our results show that temperature activation of dTrpA1 channels in octopamine neurons causes a large rise in resting potential and a substantial increase in the amplitude of the responses to visual motion during quiescence (Figure 2.5). Both effects were completely
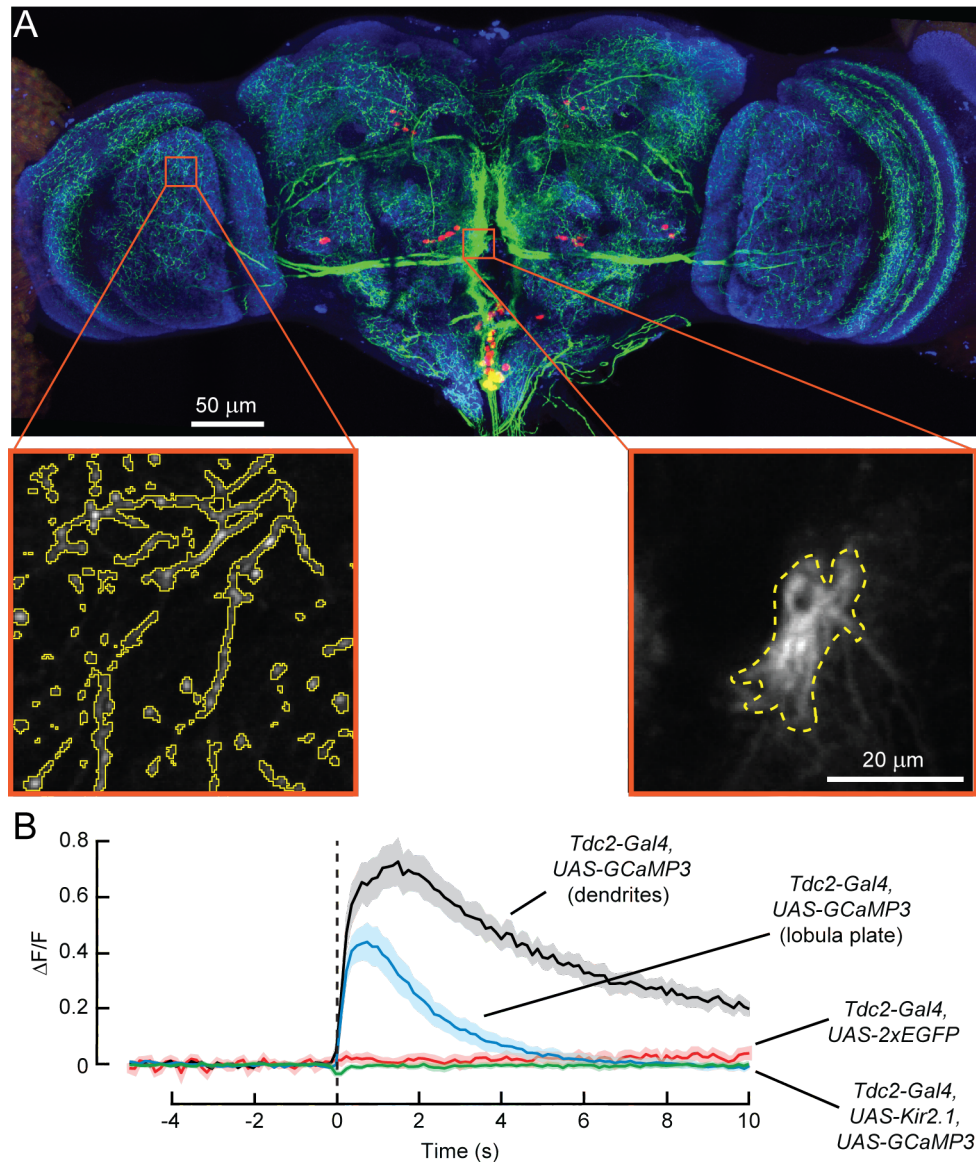
Figure 2.4: Octopamine neurons increase in activity during flight. (A) Expression pattern of *Tdc2-Gal4/ y, w, UAS-mCD8GFP ; UAS-red stinger;* , which labels processes and cell nuclei of octopamine neurons. Processes of octopamine neurons are shown in green, their cell nuclei are shown in red, and anti-nc82 staining labels neuropil in blue. We recorded calcium activity from octopamine neuron terminals in the lobula plate (location indicated by orange box on left) and in the overlapping dendrites of these same neurons (indicated by orange box on right). These regions have been expanded below. Yellow solid and dotted lines indicate regions where responses were recorded. (B) Average change in fluorescence relative to the baseline fluorescence in the regions indicated in A in flies expressing either GCaMP3 (black, dendritic response, N = 7 flies, and blue, lobula plate terminal response, N = 7 flies), 2xEGFP (red, N = 5 flies), or both GCaMP3 and Kir2.1 (green N = 5 flies, lobula plate terminal response) in octopamine neurons. Dotted line at time zero indicates when flight started, and each fly included in these averages flew for at least 10 s (longer flight bouts not shown here). Standard error about the mean is indicated in light grey, light blue and light red.

reversible upon restoration of the saline temperature to 19℃. In addition, I found that flight induced no further baseline shift (two-tailed Student's t-test; P = 0.002) or increase in visual response to motion (Figure 2.11) during activation of dTrpA1 channels. To control for possible non-specific effects of heat, I recorded VS cell responses from the two parental strains required for the dTrpA1 experiments using the same protocol. Fewer of the control flies spontaneously initiated flight upon elevation of saline temperature (4 of 12 control flies vs. 6 of 10 experimental flies). Not surprisingly, the elevation of temperature from 19° to 28° did cause some changes in cell physiology. In particular, I measured increases of 6.1 mV +/- 4.1 S.D. and 7.4 mV +/- 2.5 S.D. in the baseline membrane potential in the *Tdc2-Gal4* and *UAS-dTrpA1* parental lines, respectively, during the temperature shift. These upward shifts in baseline membrane potential did not differ significantly from the baseline shift observed in *Tdc2-Gal4/UAS-dTrpA1* flies (two-sample t-test; *Tdc2-Gal4*, P = 0.42, *UAS-dTrpA1*, P = 0.93; Figures 2.5B and 2.5C). Despite the large upward baseline membrane potential shift during elevated temperature, I observed little to no increase in the visual response to downward motion at most speeds (paired Student's t-test; significant increases found in *Tdc2-Gal4*: 2Hz P = 0.006, 4Hz P = 0.001, and in *UAS-dTrpA1*: 4 Hz P = 0.035). Of the speeds at which the control flies displayed a visual response increase at elevated temperature, each was significantly smaller than that observed in the *Tdc2-Gal4/UAS-dTrpA1* flies during downward motion with an exception at 2 Hz, where the difference was less pronounced (two-sample t-test; P = 0.13). Thus, I conclude that activation of dTrpA1 in the octopamine neurons induces a change in VS cell physiology that mimics the visual boost observed in flight and cannot be explained by non-specific temperature effects. These results suggest that whereas octopaminergic neurons may not be responsible for the flight-induced shift in baseline membrane potential, they are sufficient to produce the increased gain in visual responses.
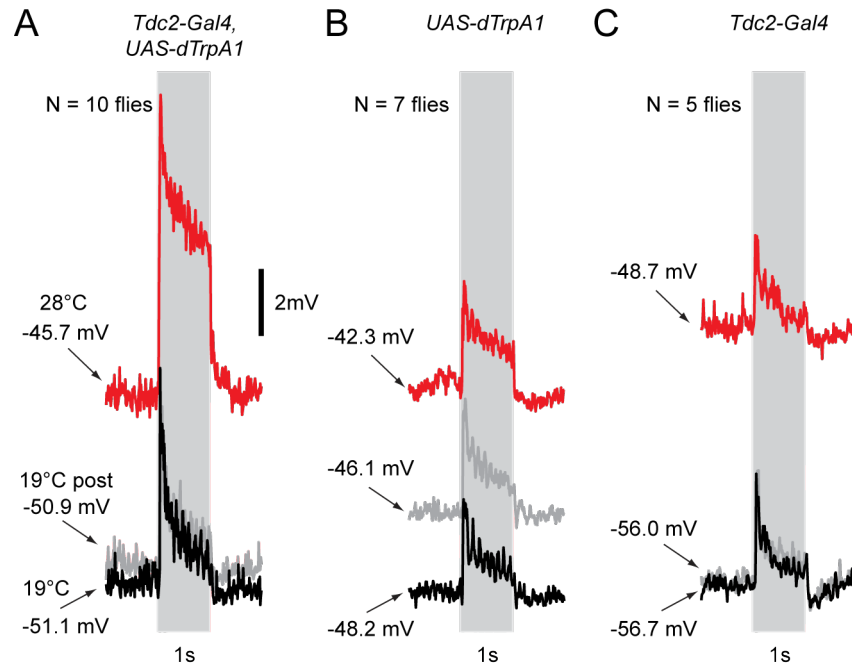
Figure 2.5: Activation of octopamine neurons increases baseline membrane potential and response to motion. (A) Average visual response to 8 Hz downward motion before (19°C, black trace), during (28°C, red trace) and after (19°C post, grey trace) dTrpA1 channels were activated in octopamine cells (*Tdc2-Gal4, UAS-dTrpA1*). Shaded light grey region indicates when the visual stimulus was in motion. Average baseline membrane potential during the 1 s immediately before motion onset is shown for each of these three conditions. (B) Average visual response to 8 Hz downward motion for parental control flies *UAS-dTrpA1*, before, during, and after temperature shift. Same scale as A. (C) Average visual response to 8 Hz downward motion for parental control flies *Tdc2-Gal4*, before, during, and after temperature shift. Same scale as A and B.
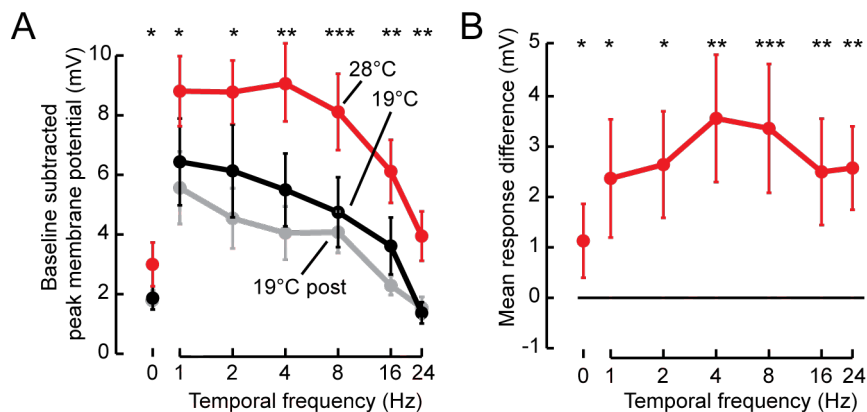
Figure 2.6: Activation of octopamine neurons induces flight boost. (A) Temporal frequency tuning curve for downward motion responses before (19°C, black trace), during (28°C, red trace), and after (19°C post, grey trace) dTrpA1 activation of octopamine cells (*Tdc2-Gal4, UAS-dTrpA1*). (B) Average response difference between during (28°C) and before (19°C) dTrpA1 activation. In A and B, responses were computed in the same manner as in Figure 2.1. Asterisks indicate speeds at which the difference between during (28°C) and before (19°C) dTrpA1 activation responses (computed for each fly) were significantly greater than zero (paired Student's t-test). Single, double, and triple asterisks indicates significance at alpha = 0.05, 0.01, and 0.001, respectively.

2.3.5 Inactivation of octopamine neurons abolishes flight-dependent visual response increase

Once I established that the activation of octopamine neurons was sufficient to produce an increase in the motion responses of VS cells, I tested the necessity of these neurons in modulating the visual response to motion during flight by expressing the inwardly-rectifying potassium channel Kir2.1 in octopamine neurons using the *Tdc2-Gal4* driver line. First, to test whether chronic expression of Kir2.1 was having the desired effect on the octopamine neurons, I examined the *Tdc2-Gal4/UAS-Kir2.1-EGFP* flies for the expected egg-laying deficit induced by the lack of octopamine (Monastirioti et al., 1996) and found that, indeed, the *Tdc2-Gal4/UAS-Kir2.1-EGFP* flies were unable to lay eggs (data not shown). Flies with chronically inactivated octopaminergic neurons were, however, both viable and able to fly, consistent with a previous study of an octopamine null mutant (Brembs et al., 2007). During flight, VS cells showed no significant difference in upward shift in baseline membrane po-
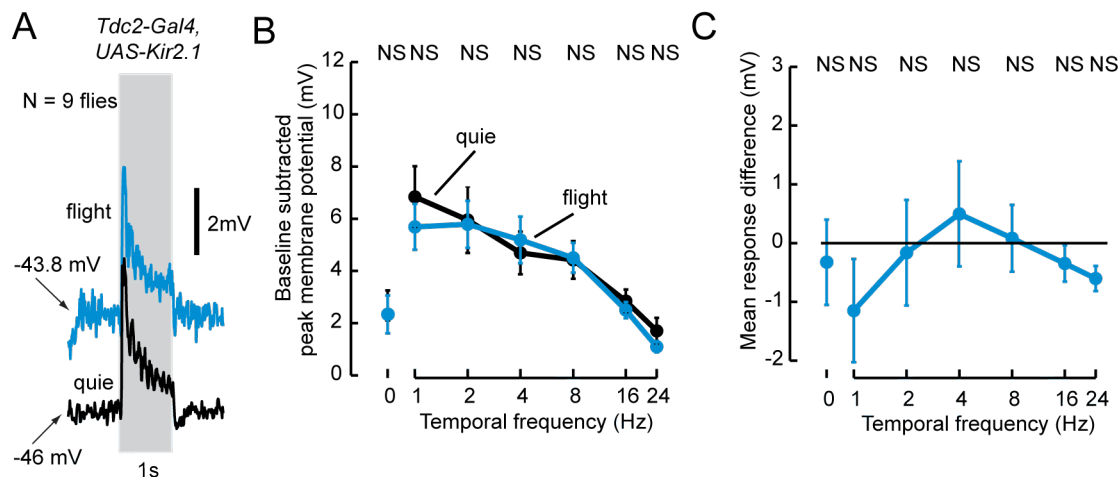
Figure 2.7: Inactivation of octopamine neurons abolishes flight boost. (A) Average visual response to 8 Hz downward motion during quiescence ('quie', black trace) and flight (blue trace) in flies whose octopamine neurons are inactivated by Kir2.1 (*Tdc2-Gal4, UAS-Kir2.1*). Grey region indicates when the visual stimulus was in motion. Average baseline membrane potential during the 1 s immediately before motion onset is shown for quiescence and flight. (B) Temporal frequency tuning curve for downward motion responses during quiescence and flight for flies whose octopamine neurons were inactivated (*Tdc2-Gal4, UAS-Kir2.1*). (C) Difference between flight and quiescent responses for flies whose octopamine neurons were inactivated (*Tdc2-Gal4, UAS-Kir2.1*). In B and C, responses were computed in the same manner as in Figure 2.1. NS indicates speeds at which the difference between flight and quiescent responses (computed for each fly) were not significantly greater than zero (alpha $<= 0.05$, paired Student's t-test).

tential compared to wild-type flies (two-sample t-test, P = 0.63), which suggests that while pharmacological application of octopamine can mimic this effect (Figure 2.2), this change in cell physiology during flight does not require the activity of octopamine neurons. This result is also in agreement with the evidence from our dTrpA1-activation experiments, which did not support that octopamine neurons are involved in producing the DC shift observed during flight. However, VS cells in flies with inactivated octopamine cells displayed an impaired visual boost during flight (Figure 2.7A, 2.7C and 2.7D). Furthermore, *UAS-Kir2.1-EGFP* parental control flies showed a clear boost during flight (Figure 2.7B, 2.7E and 2.7F). These experiments indicate that octopamine neurons are not simply sufficient but also necessary for the flight-dependent increase in visual motion gain of VS cells.
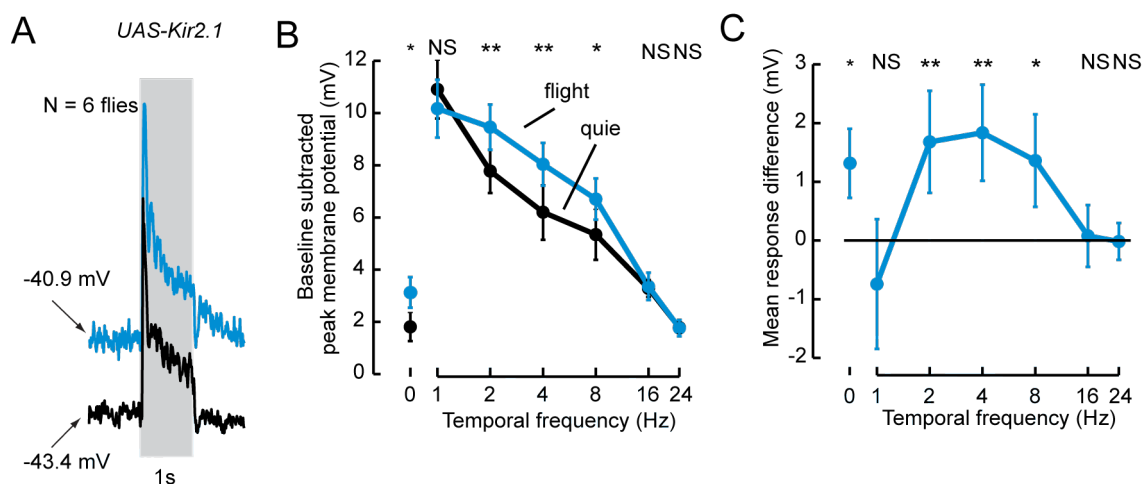
Figure 2.8: Background control flies for Kir inactivation experiment (see Figure 2.7) show normal flight effects. (A) Average visual response to 8 Hz downward motion during quiescence ('quie', black trace) and flight (blue trace) for *UAS-Kir2.1* parental background control flies. Grey region indicates when the visual stimulus was in motion. Average baseline membrane potential during the 1 s immediately before motion onset is shown for quiescence and flight. (B) Temporal frequency tuning curve for downward motion responses during quiescence and flight for *UAS-Kir2.1* control flies. (C) Difference between flight and quiescent responses for *UAS-Kir2.1* control flies. In B and C, responses were computed in the same manner as in Figure 2.1. Asterisks indicate speeds at which the difference between flight and quiescent responses (computed for each fly) were significantly greater than zero (paired Student's t-test). Single and double asterisks indicates significance at alpha = 0.05 and 0.01, respectively. NS indicates no significance at alpha $<= 0.05$.

2.4 Discussion

In this chapter I presented evidence that octopamine neurons play a key role in the modulation of large field visual interneurons during flight. I characterized the motion response of VS cells during flight across a broad range of temporal frequencies, and found that the boost in visual gain is variable across speeds (Figure 2.1), consistent with previous studies in walking and flying flies (Chiappe et al., 2010; Jung et al., 2011). Exogenous application of octopamine replicates many features of the change in VS cell physiology observed during flight (Figure 2.3). This result supports the findings of previous extracellular studies in blowflies that reported an increase in the response gain of other lobula plate tangential cells after pharmacological application of the octopamine agonist chlordimeform (Jung et al., 2011; Longden and Krapp, 2009, 2010). Although these pharmacological experiments are suggestive of a role of octopamine in modulating visual responses during flight, it is important to demonstrate that the endogenous system of octopamine neurons is actually responsible for the effect. By using GCaMP3 to monitor activity, we found that the octopamine neurons with dense innervations in the optic lobes do indeed increase in activity at the onset of flight (Figure 2.4). When I activated the octopamine neurons via ectopically-expressed dTrpA1, these neurons evoke a very large increase in the VS cell responses to visual motion in quiescent flies (Figure 2.5), indicating that the activation of octopamine neurons is sufficient to generate the effect. The complementary experiment, in which I inactivated octopamine neurons using Kir2.1 (Figure 2.7), demonstrated that these neurons are also necessary to produce the flight boost. Figure 2.9 shows a summary of the average responses for each experimental condition and control.

Our activation and inactivation experiments suggest that the octopamine neurons play a major role in producing the flight boost observed in VS cells. The activity of two different regions of these neurons, the dendrites and output terminals in the lobula plate, appears to be somewhat different, and raises questions about the dynamics of octopamine neurons relative to the flight boost. In the lobula plate, these neurons produced a smaller increase in fluorescence during flight, relative to their input re-
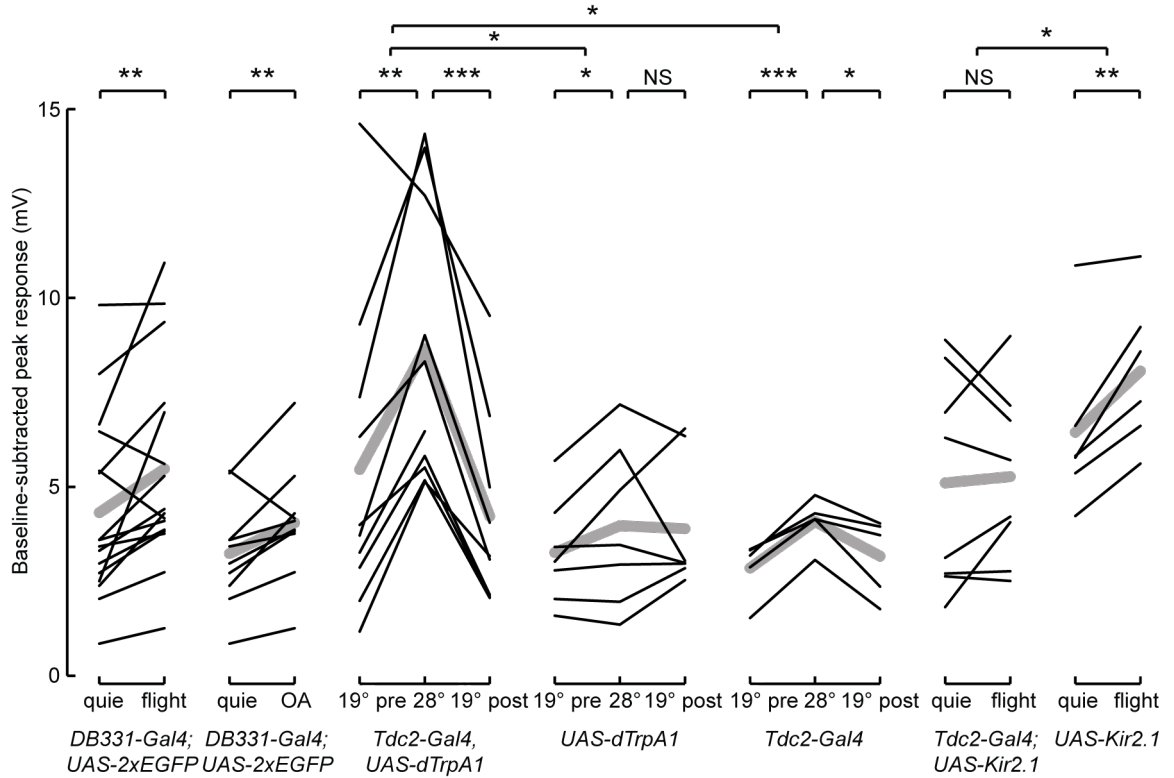
Figure 2.9: Cross-condition summary. Average baseline-subtracted peak response across the three middle temporal frequencies at which the flight boost is significant (2, 4 and 8 Hz, see Figure 2.1). A single fly's average within each condition is shown (black points connected by lines). Grey lines indicate the population mean within each condition. All values listed in degrees were measured in Celsius. Bottom row of asterisks indicate speeds at which responses during flight, octopamine application, or dTrpA1 activation at 28°C are significantly higher than the pre-condition responses (quiescence or before dTrpA1 activation [19° pre]; paired Student's t-test). Upper rows of asterisks indicate when the difference during one condition is significantly higher than the difference observed in the other (two-sample t-test). Single, double, and triple asterisks indicates significance at alpha = 0.05, 0.01, and 0.001, respectively. NS indicates no significance at alpha <= 0.05.

gion. In addition, these output region responses decayed more rapidly, reaching close to zero by about six s into a flight bout (Figure 2.4). Given this decay in activity after a few seconds, how do octopamine neurons mediate long-lasting increases in response to visual motion in VS cells throughout a long flight bout (Maimon et al., 2010)? It is possible that these neurons release octopamine at the beginning of flight, and this produces long-lasting changes in VS cells. This could be mediated by intracellular second messenger systems initiated by octopamine receptors, for example. Alternatively, the octopamine neuron output processes might be weakly active throughout a long flight bout, but are underrepresented in our measure because GCaMP3 fluorescence is nonlinear with respect to free calcium concentration (Tian et al., 2009). A third possibility is that the GCaMP3 signal in this experiment accurately reports a decrease in activity of octopamine neuron processes in the lobula plate, but these cells remain active in other parts of the visual system and modulate upstream elements continuously during a flight. Future experiments targeting upstream elements, intracellular signaling mechanisms, or the development of more sensitive calcium indicators may help to shed light on this discrepancy. Regardless of how the octopamine neurons might mediate the flight boost over long flight bouts, our experiments support that octopamine neurons become active during flight (Figure 2.4) and are necessary for this effect (Figure 2.7).

These experiments do not, however, support a role for octopamine in causing the tonic membrane potential shift. When the octopamine neurons were silenced with Kir2.1, VS cells still exhibited a rapid shift in membrane potential at the onset of flight (Figure 2.7). Further, although I did measure a large baseline shift in our dTrpA1 activation experiments, a comparison with control experiments using the two parental stocks suggests that this effect – but not the change in response gain – is an artifact of the elevated temperature (Figure 2.5). These results, together with the previous observation that the two effects follow different time courses at the onset and offset of flight (Maimon et al., 2010), suggest that the upward shift in membrane potential and the increase in the visual response to motion are generated by two distinct mechanisms. At odds with this conclusion is our observation of an
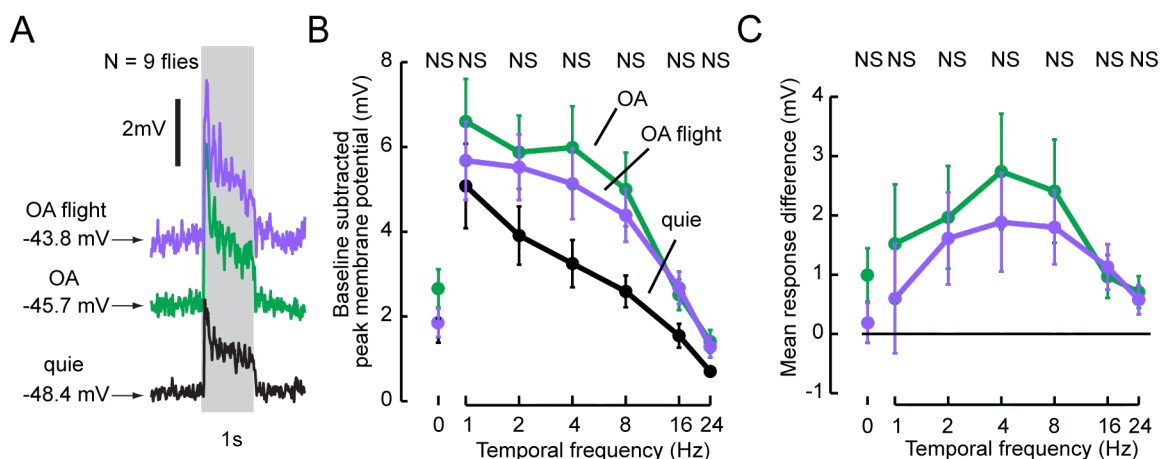
Figure 2.10: Effect of flight during octopamine application. (A) Average visual response to 8 Hz downward motion during quiescence ('quie', black traces), octopamine application (OA; green trace) and flight during octopamine application (OA flight; purple trace). The grey shaded region indicates when the visual stimulus was in motion. The average baseline membrane potential during the 1 s immediately before motion onset is shown for quiescence, OA and OA flight. (B) Temporal frequency tuning curve for downward motion responses during quiescence, octopamine application, and flight during octopamine application. Abscissa is plotted on a log scale. (C) Difference between motion responses during octopamine application and quiescence, and flight during octopamine application and quiescence. Abscissa is plotted on a log scale. In B and C, NS indicates speeds at which the difference between OA flight responses and OA responses (computed for each fly) was not significantly greater than zero (paired Student's t-test, alpha = 0.05).

upward baseline shift in VS cells during pharmacological application of octopamine (Figure 2.3). Pharmacological application of the octopamine agonist chlordimeform has also been shown to cause an increase in spontaneous firing rate in a lobula plate tangential neurons in blowflies (Jung et al., 2011; Longden and Krapp, 2009, 2010), which is consistent with our findings, but unfortunately offers no further insight into why the baseline shift persisted when the octopamine cells were silenced with Kir2.1.

One possible explanation for why silencing octopamine cells abolished the flight boost but not the baseline shift is that our manipulation of cell activity might not be uniform across all cells in the *Tdc2-Gal4* line. Variable expression of the driver, or alternatively, variable activation of the responder, might have resulted in heterogeneous inactivation of octopamine neurons by Kir2.1. In this scenario, the octopamine neurons involved in both egg-laying behavior and the visual boost were substantially

inactivated by Kir2.1, but the octopamine neurons responsible for the baseline shift were active enough to induce a baseline shift during flight. However, this explanation is feasible only if the baseline shift is mediated by octopamine neurons, and the time course of the baseline shift, which occurs instantaneously at the onset of flight (Maimon et al., 2010), is not entirely consistent with the action of a neuromodulator. The four known neuronal octopamine receptors in *Drosophila* are all G-protein coupled receptors (Evans and Maqueira, 2005), whose actions may act on a much slower time scale (Siegelbaum and Tsien, 1983) relative to the baseline shift we record at the onset of flight. For this reason, I believe it unlikely that octopamine is responsible for the baseline shift and think it improbable that heterogeneity in the effect of Kir2.1 across the population of octopamine cells can explain the discrepancy. An alternative explanation is that pharmacological application of octopamine throughout the brain induces general effects that are manifest as an upward shift in membrane potential in VS cells, but that this shift is biophysically distinct from the shift that occurs during flight. During flight, octopamine might be released at very specific sites in the optic lobes. Activation and inhibition of octopamine cells will induce or abolish the flight boost, respectively, but have no effect on the baseline membrane potential in this scenario. Pharmacologically-applied octopamine reaches many regions throughout the brain that are not typically supplied with this neuromodulator, and this may result in broad nonspecific effects. This might include, for example, cross-reactivity with various non-octopamine receptors or ion channels that cause a shift in baseline membrane potential. There are many mechanisms by which a neuron's resting membrane potential can be increased, and various biogenic amines have been shown to affect multiple physiological targets (Flamm and Harris-Warrick, 1986b). Although further experiments are required to resolve the issue, I believe that such nonspecific effects are the most likely cause of the membrane potential shift observed in VS cells during exogenous application of octopamine, and that octopamine neurons are not responsible for the baseline shift observed during flight. This hypothesis is strengthened by the observation that during octopamine application, flight induces an additional shift of baseline membrane potential but no further visual boost (Figure 2.10). Similarly,

during dTrpA1 activation of octopamine neurons, flight induces no additional visual boost (Figure 2.11), suggesting that the cell's response is saturated. Flight did not significantly alter the baseline membrane potential during dTrpA1 activation, but based on control experiments, it is clear that heat is responsible for a very large baseline shift that may obscure any further small increase induced by flight. Collectively, I believe that these data support the hypothesis that octopamine neurons underlie the visual boost but not the baseline shift.
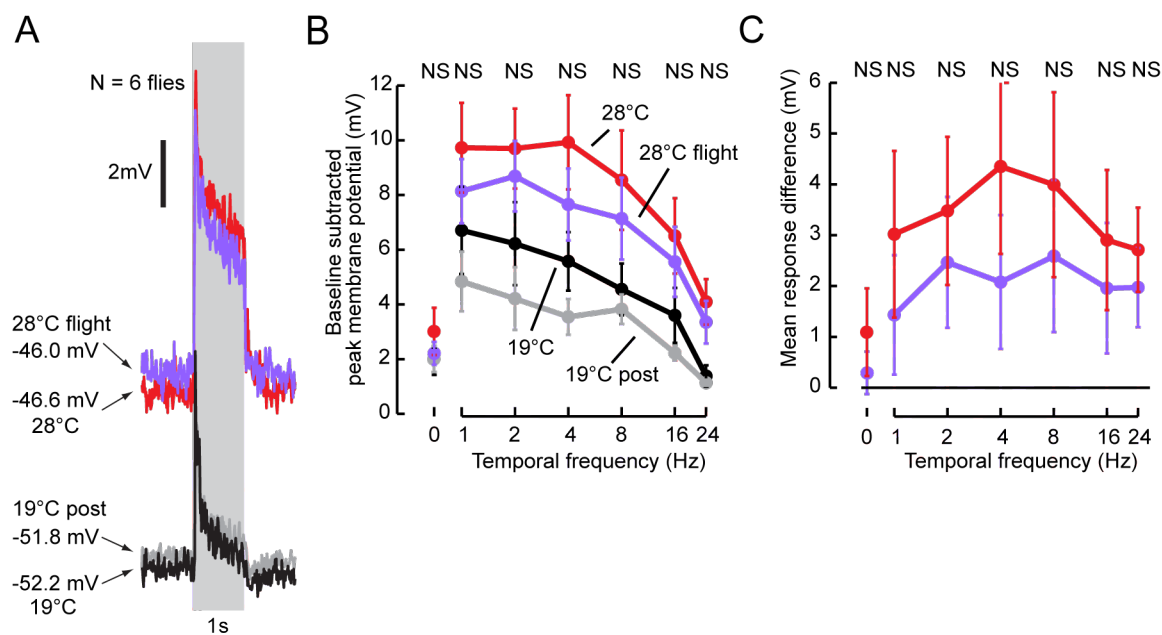
Figure 2.11: Effect of flight during activation of octopamine neurons. (A) Average visual response to 8 Hz downward motion before (19°C, black trace), during (28°C, red trace), during while flying (28°C flight, purple trace), and after (19°C post, grey trace) dTrpA1 channels were activated in octopamine cells (*Tdc2-Gal4, UAS-dTrpA1*). Shaded light grey region indicates when the visual stimulus was in motion. Average baseline membrane potential during the 1 s immediately before motion onset is shown for each of these four conditions. (B) Temporal frequency tuning curve for downward motion responses before, during, during while flying, and after dTrpA1 activation. (C) Average response difference between during (28°C) and before (19°C) dTrpA1 activation, and between during while flying (28°C flight) and before (19°C) dTrpA1 activation. In B and C, NS indicates speeds at which the difference between 28°C flight responses and 28°C responses (computed for each fly) was not significantly greater than zero (paired Student's t-test, alpha = 0.05).

Chapter 3

Genetic manipulation of the lobula-plate projecting octopamine neurons

3.1   Introduction

In Chapter 2, I showed that octopamine neurons were responsible for the flight-induced increase in visual responses to motion in VS cells. We found that the group of octopamine neurons that project to the optic lobes become active during flight (Figure 2.4), and the entire set of octopamine neurons is necessary and sufficient for the flight boost (Figures 2.5, 2.6, and 2.7). It remained unclear, however, what the contribution of individual octopamine neurons was in the flight boost observed in VS cells. The cell bodies of the six optic-lobe projecting neurons are located near the midline, near the esophagus foramen and the antennal lobes. These cell bodies are accessible for electrophysiological recordings, but not in a preparation that also permits flight behavior (see also Section 2.5). However, through a collaboration with the Kravitz lab at Harvard University, I was able to manipulate octopamine neuron activity using a reproducible enhancer trap line that labels a single pair of octopamine neurons that project to the optic lobes (Figure 3.1), which I will call Kravitz line 243. Based on its pattern of optic lobe innervation, I believe that this neuron is the OA-AL2i1 neuron, whose stereotyped morphology is described in detail in Busch et al. (2009), and refer to it as such for the remainder of this thesis. This neuron is the only
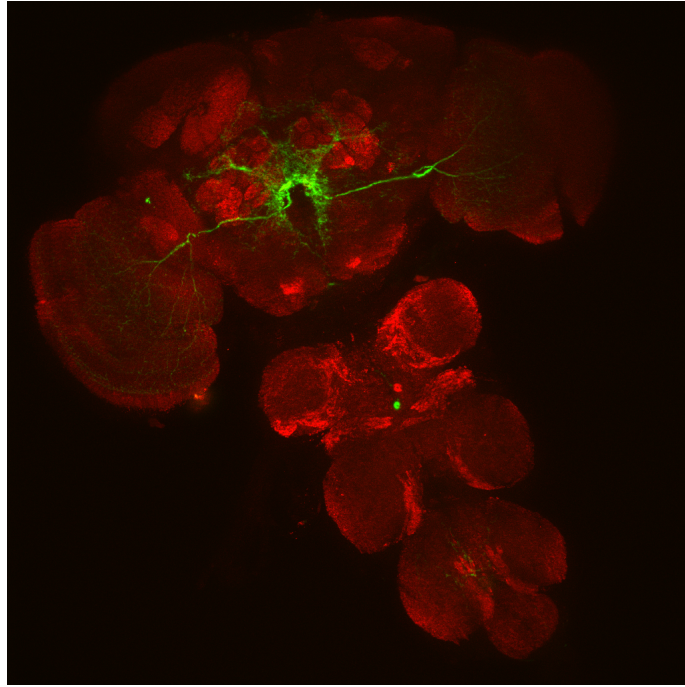
Figure 3.1: Expression pattern of a single pair of octopamine neurons labeled by the combinatorial driver line *Tdc2-Gal4;243-FLP*. Processes of octopamine neurons are shown in green and anti-nc82 staining labels neuropil in red. Image courtesy of Kyle Gobrogge, Kravitz lab, Harvard University.

octopaminergic neuron that innervates the lobula plate directly, making it a good candidate for mediating the changes I observe in VS cells during flight. I first blocked synaptic transmission in this pair of neurons using tetanus toxin light chain (TNT), and observed no effect on the flight boost in VS cells. Next, I manipulated the activity of this pair of neurons using dTrpA1 and found weak evidence that activation of these neurons increases the activity of VS cells in a manner similar to that observed during flight.

3.2 Experimental procedures

All experimental procedures, including animals, solutions, data analysis and statistics, were performed in the manner described in Chapter 2, with any exceptions listed below.

3.2.1   Animals

Flies were generously donated by the Kravitz lab at Harvard University. To label subsets of octopamine neurons, a set of enhancer-trap FLP recombinase transgenic lines was first produced. Next, by driving expression of Gal4 using the panneuronal *elav-Gal4* driver in combination with these lines, expression of GFP (using *UAS>stop>mCD8::GFP*) was restricted to subsets of neurons in the brain – only neurons expressing both the FLP recombinase and Gal4 expressed GFP. The lines were then screened for reliable GFP expression. Expression was further restricted in the brain by combining the reliably-expressing enhancer-trap FLP lines with the *Tdc-Gal4* driver line, which alone labels all octopamine neurons. One of the reproducible enhancer trap lines generated, line 243 (*;Tdc2-Gal4;243-flipase*), together with the *Tdc-Gal4* driver line, label a single pair of octopamine neurons that project to the optic lobes. I used this combinatorial driver line (*Tdc2-Gal4;243-FLP*) to drive expression of various effector proteins. Reproducibility was high in this line - at least 95% of all brains examined expressed GFP in the same two neurons (Dr. Kyle Gobrogge, personal communication). To manipulate neuronal activity, either tetanus toxin light chain (TNT, Sweeney et al., 1995) or dTrpA1 (Hamada et al., 2008) was expressed in this pair of neurons using the following constructs: *UAS>stop>TNT* and *UAS>stop>dTrpA1* (full genotypes are *;UAS>stop>TNT;+* and *w[*];UAS>stop>dTRPA1;+*, respectively). See Alekseyenko et al. (2013) for more details about the enhancer-trap FLP screening method.

3.2.2   Whole cell patch clamp recordings

I used electrodes with resistance of 4.7-7.1 MΩ. Our intracellular, external, and collagenase solutions were identical to those used in Maimon et al. (2010). The average resting potential of cells after compensation for an experimentally-measured junction potential (-13mV) was -46.5mV. I injected 20-30pA constant hyperpolarizing current into the cells prior to presentation of visual stimuli to aid with dye fills, which decreased the membrane potential by an average of -3.9mV (to -50.5 mV). The access

resistance (R_{acc}) for all recordings was 28.7 $+/-$ 6.9 MΩ S.D.. See Chapter 2 for additional recording methods.

3.3 Results

3.3.1 Blocking chemical synaptic transmission in the octopamine neuron OA-AL2i1 has no effect on flight boost

I first tested if the OA-AL2i1 neuron was necessary for producing the flight boost observed in VS cells. To do so, I looked for an available *UAS>stop>effector* line that would decrease neuronal activity. Expression of the inward-rectifying potassium channel Kir2.1 is an effective way of inhibiting neuronal activity (Johns et al., 1999; Baines et al., 2001, see also Section 2.7), however, at the time I performed these experiments, a *UAS>stop>Kir2.1* line was not available to inhibit activity of these neurons. Instead, I employed a *UAS>stop>TNT* construct, which encodes tetanus toxin light chain (TNT), a blocker of chemical synaptic transmission (Sweeney et al., 1995).

When I expressed TNT in the OA-AL2i1 neurons, I observed no clear deficit in the flight boost as measured in VS cells (Figure 3.2 and 3.5). In addition, I found that although the baseline shift of TNT flies was smaller than wild-type flies, it was not significantly so (Figure 3.2A and B; two sample t-test, P = 0.11). These results suggest that the flight boost may not mediated by synaptic transmission via the OA-AL2i1 neurons. However, there is some evidence that suggests that TNT expression is temperature dependent (Jösch Krotki, 2009), so it is also possible that we did not fully block synaptic transmission in this pair of octopamine neurons.
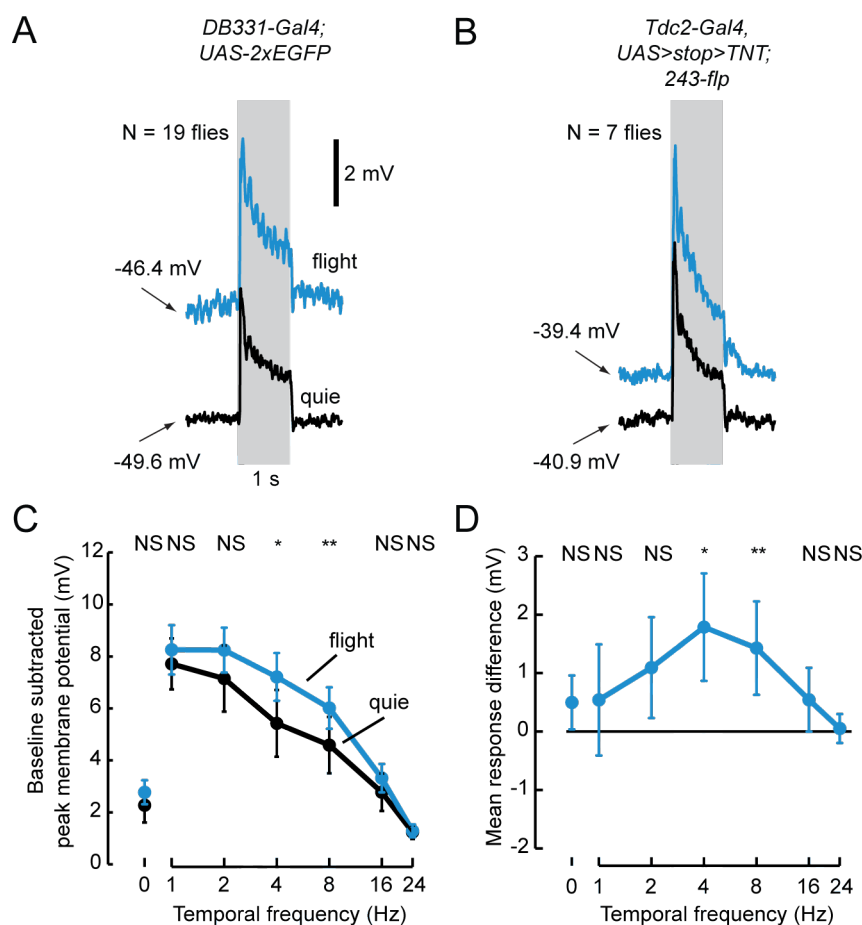
Figure 3.2: Expression of TNT in one octopamine neuron has no effect on the flight boost. (A) Average VS cell visual responses to 8 Hz downward motion during quiescence ('quie', black traces) and flight (blue traces) (data from Figure 2.1B). (B) VS cell responses from flies whose octopamine neurons express tetanus toxin (*Tdc2-Gal4, UAS>stop>TNT; 243-FLP*) during quiescence (black traces) and flight (blue traces). The grey region indicates when the visual stimulus was in motion. Average baseline membrane potential during the 1 s immediately before motion onset is shown for quiescence and flight. Same scale as A. (C) Temporal frequency tuning curve for downward motion responses during quiescence and flight for flies in which OA-Al2i1 neuron synaptic activity was blocked (*Tdc2-Gal4, UAS>stop>TNT; 243-FLP*). (D) Difference between flight and quiescent responses for flies in which OA-Al2i1 neuron synaptic activity was blocked (*Tdc2-Gal4, UAS>stop>TNT; 243-FLP*). In C and D, responses were computed in the same manner as in Figure 2.1. Asterisks indicate speeds at which the difference between flight and quiescent responses (computed for each fly) were significantly greater than zero (paired Student's t-test). Single and double asterisks indicates significance at alpha = 0.05 and 0.01, respectively. NS indicates no significance at alpha <= 0.05.

3.3.2   Heat induces an increase in VS cell responses to motion in *UAS>stop>dTrpA1* control flies

The entire set of octopamine neurons are sufficient to induce the visual boost in VS cells (Chapter 2.6), and although synaptic inactivation of the single pair of OA-AL2i1 neurons had no effect on the flight boost, it remained unclear if these cells alone be sufficient to produce this effect. I activated the OA-AL2i1 neurons by genetically expressing the heat sensitive cation channel dTrpA1 (using the *UAS>stop>dTrpA1* construct and Kravitz line 243) and observed similar results as when I activated the entire set of octopamine neurons using the *Tdc2-Gal4* driver line – both the visual response to motion and the baseline membrane potential increased (Figure 3.3 and 3.4). However, the visual response increase I observed in the experimental flies was larger, but not significantly so, than that observed in the parental strain, *UAS>stop>dTrpA1* (Figure 3.3 and 3.5). It may be possible that the visual responses of this genetic background are more susceptible to nonspecific heat effects than other genetic backgrounds (see Section 2.6) or that the *UAS>stop>dTrpA1* construct is leaky. Without a larger sample size or additional experiments, the strong heat effect in this parental line background undermines any conclusions I might make about the effect of activating the OA-AL2i1 neuron.

3.3.3   Genetic background and the effect of heat on VS cell responses

The relatively large heat effect in the *UAS>stop>dTrpA1* parental control flies discussed in Section 3.3.2 left us questioning whether the *UAS>stop>dTrpA1* construct was leaky, or if there exist large differences between the effects of heat in VS cells across various genetic backgrounds. In an effort to gain some insight about this issue, I compared the effect of heat across a number of genetic backgrounds. In addition to the two parental heat controls from Chapter 2 (Section 2.6, also see Figure 2.5), and
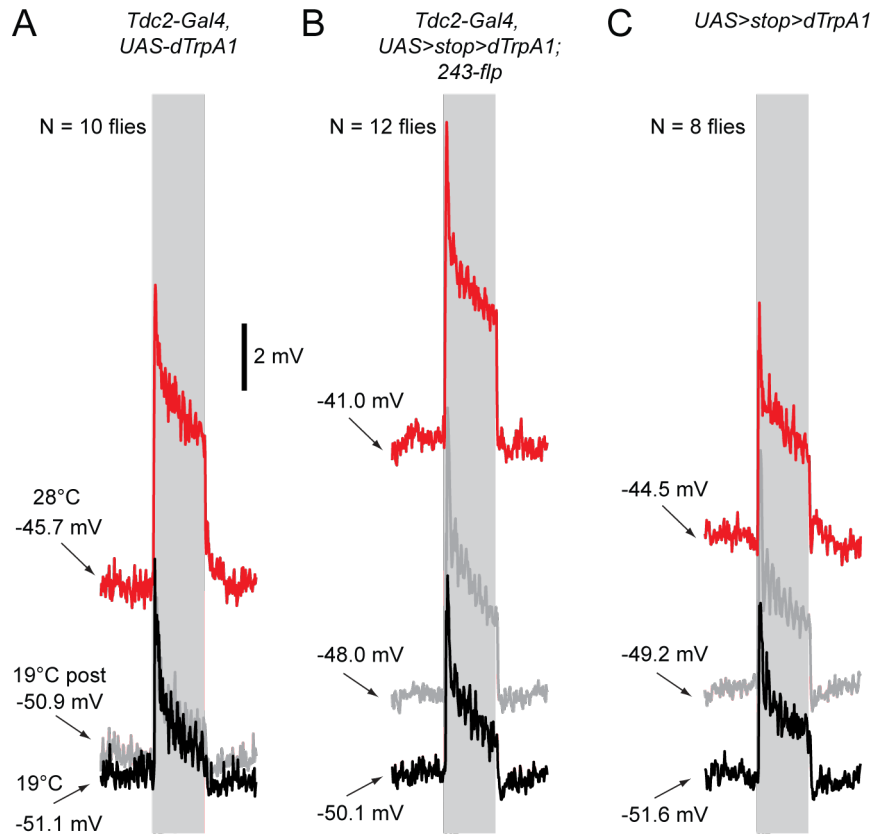
Figure 3.3: Expression of dTrpA1 in one octopamine neuron may increase VS cell responses to motion. (A) Average visual response to 8 Hz downward motion before (19°C, black trace), during (28°C, red trace) and after (19°C post, grey trace) dTrpA1 channels were activated in all octopamine cells (*Tdc2-Gal4, UAS-dTrpA1*; Data from Figure 2.5A). Shaded light grey region indicates when the visual stimulus was in motion. Average baseline membrane potential during the 1 s immediately before motion onset is shown for each of these three conditions. (B) Average visual response to 8 Hz downward motion when dTrpA1 channels were expressed in a single pair of octopamine cells (*Tdc2-Gal4, UAS-dTrpA1; 243-flp*), before, during, and after temperature shift. Same scale as A. (C) Average visual response to 8 Hz downward motion for parental control flies *UAS>stop>dTrpA1*, before, during, and after temperature shift. Same scale as A and B.
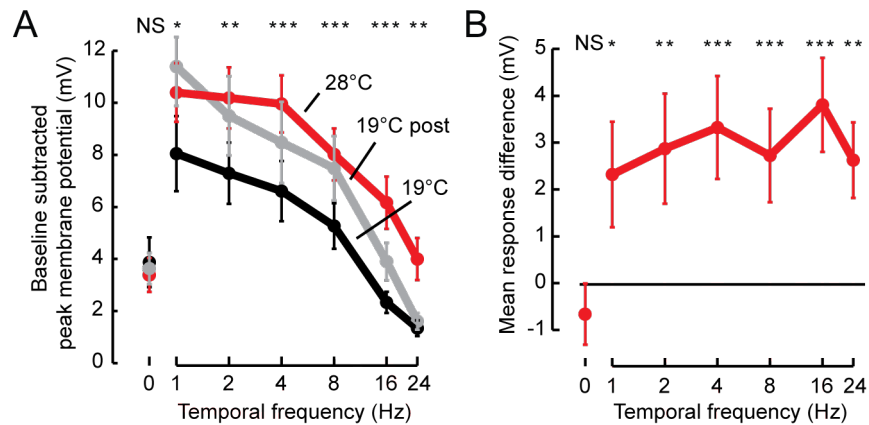
Figure 3.4: Expression of dTrpA1 in one octopamine neuron type may increase VS cell responses to motion across a range of temporal frequencies. (A) Temporal frequency tuning curve for downward motion responses before (19°C, black trace), during (28°C, red trace), and after (19°C post, grey trace) dTrpA1 activation the single pair of octopamine neurons labeled by Kravitz line 243 (*Tdc2-Gal4, UAS-dTrpA1; 243-flp*). (B) Average response difference between during (28°C) and before (19°C) dTrpA1 activation. In A and B, average responses were computed in the same manner as in Figure 2.1, across the N = 10 flies in Figure 3.3B. Asterisks indicate speeds at which the difference between during (28°C) and before (19°C) dTrpA1 activation responses (computed for each fly) were significantly greater than zero (paired Student's t-test). Single, double, and triple asterisks indicates significance at alpha = 0.05, 0.01, and 0.001, respectively.
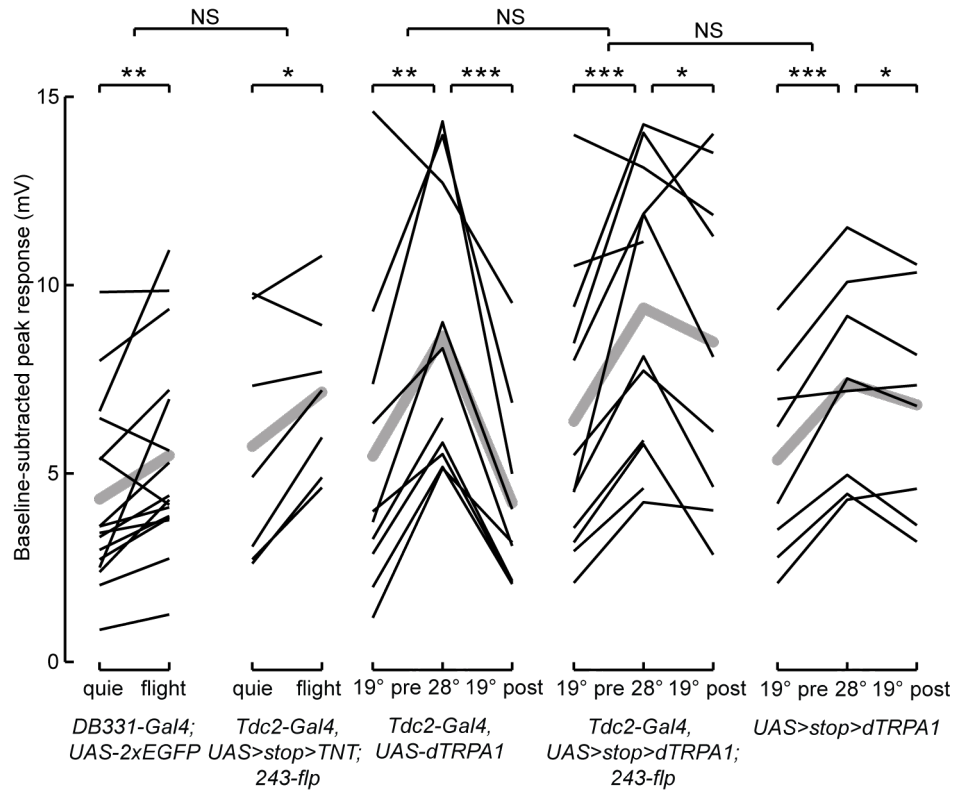
Figure 3.5: Manipulation of the OA-AL2i1 octopamine neuron - cross-condition summary. Average baseline-subtracted peak response across the three middle temporal frequencies at which the flight boost is significant (2, 4 and 8 Hz, see Figure 2.1). A single fly's average within each condition is shown (black points connected by lines). Grey lines indicate the population mean within each condition. All values listed in degrees were measured in Celsius. Bottom row of asterisks indicate speeds at which responses during application of heat are significantly higher than the pre-condition responses (before heat application [19° pre] or flight; paired Student's t-test) or when responses after heat (19° post) are significantly lower than during heat application (paired Student's t-test). Upper row indicates if the difference during one condition is significantly higher than the difference observed in the other (two-sample t-test). Single, double, and triple asterisks indicates significance at alpha = 0.05, 0.01, and 0.001, respectively. NS indicates no significance at alpha $<=$ 0.05. Data from Figure 2.9 (*DB331-Gal4, UAS-2xEGFP*; and *Tdc2-Gal4, UAS-dTrpA1*;) repeated.

DB331-Gal4;
UAS-2xEGFP

N = 5 flies

2mV

28°C
-41.6 mV

19°C post
-47.3 mV

19°C
-50 mV

1s
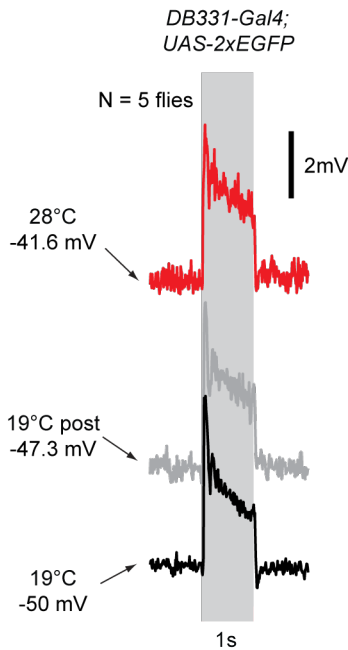
Figure 3.6: Heat does not increase VS cell responses to motion in *DB331-Gal4; UAS-2xEGFP* flies. Average visual response to 8 Hz downward motion before (19°C, black trace), during (28°C, red trace) and after (19°C post, grey trace) temperature shift. Shaded light grey region indicates when the visual stimulus was in motion. Average baseline membrane potential during the 1 s immediately before motion onset is shown for each of these three conditions.

that presented in Section 3.3.2 (Figure 3.3), I also measured the effect of heat on the visual responses of VS cells in an additional genotype, *DB331-Gal4; UAS-2xEGFP* (Figure 3.6), which are wild-type except for expression of GFP in VS cells. These flies showed no significant increase in VS cell responses to motion during heat application at any of the frequencies presented (alpha $<= 0.05$, paired Student's t-test; data not shown).

Next, I tested whether heating flies to a lower temperature at which dTrpA1 channels are still activated would lower any nonspecific heat effects I might be observing. dTrpA1 channels have been found to elicit action potentials in neurons at temperatures as low as 25°C (Hamada et al., 2008), so I performed a heat control experiment with *UAS>stop>dTrpA1* flies using this as the permissive temperature, instead of 28°C, which I used in previous experiments. When heated to 25°C, the visual responses of VS cells did not increase except at the two highest frequencies, 16 and 24Hz (two-sample t-test; P = 0.0057 and P = 0.0002, respectively). I cannot be sure that this control is useful as a comparison for activation of the OA-AL2i1 neurons, however, without verification that exogenously expressed dTrpA1 channels are also activated at this temperature. Furthermore, I have not yet verified that the response

observed in *UAS>stop>dTrpA1* flies is not the result of a leaky construct. This line has been used in only one published study to our knowledge at this time (von Philips-born et al., 2011), and unfortunately the authors did not provide evidence to support that the line is not leaky, either by showing that dTrpA1 is not produced ectopically in these flies (using qRT-PCR, for example) or by providing data demonstrating the effect of heat in this control line alone. In any case, our data show that temperature can have a variable effect on the visual responses of VS cells, and this phenomena may occur in many other cell types, and serves as an important reminder to consider the side effects of heat when using different genetic backgrounds and transgenes.

3.4   Discussion

Using a combinatorial labeling system to manipulate the activity of individual octopamine neurons, I attempted to begin dissecting the system responsible for producing the flight boost I observe in VS cells. I first blocked synaptic transmission of OA-AL2i1 neurons and observed no clear effect on the flight boost (Figure 3.2). This experiment suggests that the OA-AL2i1 neurons may transmit information via electrical synapses to the visual system, which are therefore not affected by TNT, or that they may not be involved in producing the changes I observe in VS cells during flight. Further experiments are needed to resolve which of these possibilities is most likely. Very recently, we located a *UAS>stop>Kir2.1* construct (Barry Dickson lab, personal communication), and plan to test whether inactivating OA-AL2i1 neurons completely using this construct has any effect on the VS cell flight boost.

I also found that the increase in the response to visual motion in flies whose OA-AL2i1 neurons I activated using dTrpA1 was large, but not significantly larger than that observed in control flies, which renders the contribution of this single pair of neurons to the flight boost ambiguous. The effect of heat on the visual responses of parental control flies (*UAS>stop>dTrpA1*) for this experiment was more pronounced than in other strains (Figures 3.3 and 3.7). Genetic background can introduce significant variations in responses at the cellular, system, and behavioral levels. A correct
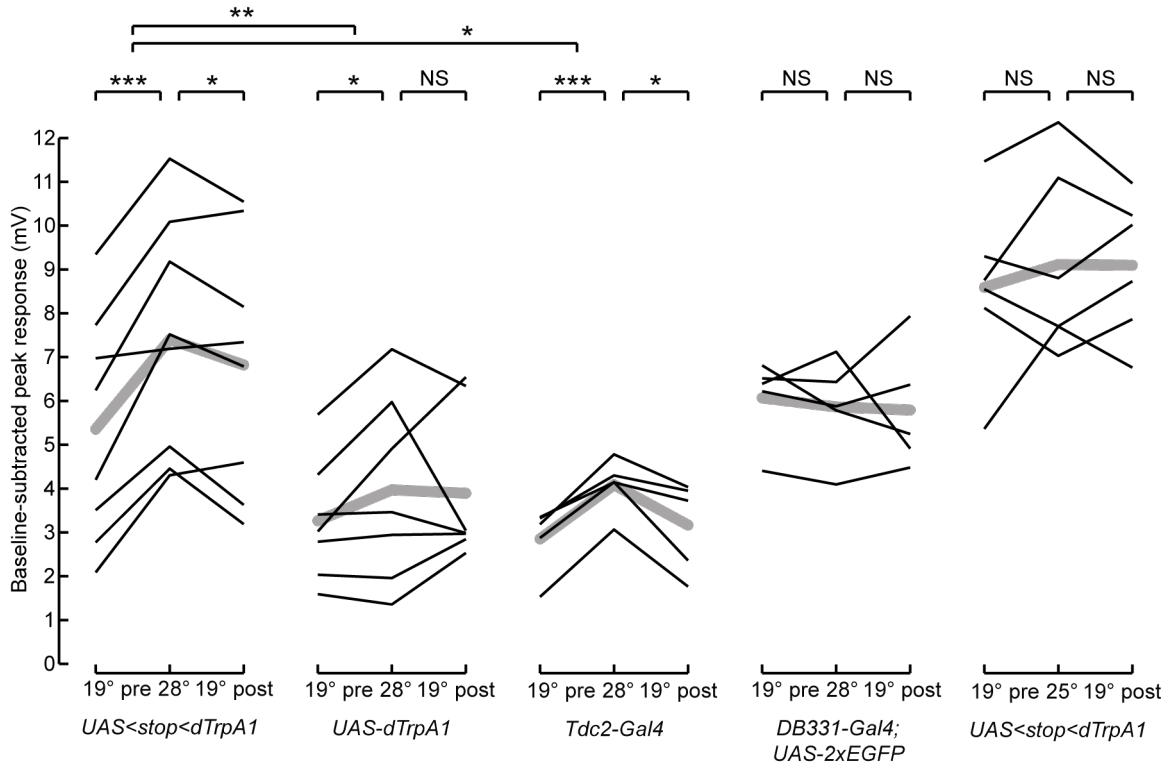
Figure 3.7: Heat effect on individual fly VS cell responses in different backgrounds. Average baseline-subtracted peak response across the three middle temporal frequencies at which the flight boost is significant (2, 4 and 8 Hz, see Figure 2.1). A single fly's average within each condition is shown (black points connected by lines). Grey lines indicate the population mean within each condition. All values listed in degrees were measured in Celsius. Bottom row of asterisks indicate speeds at which responses during application of heat are significantly higher than the pre-condition responses (befor heat application [19° pre]; paired Student's t-test). Upper rows of asterisks indicate when the difference during one condition is significantly higher than the difference observed in the other (two-sample t-test). Single, double, and triple asterisks indicates significance at alpha = 0.05, 0.01, and 0.001, respectively. NS indicates no significance at alpha <= 0.05.

interpretation of genetic manipulations such as those used in this chapter depend on the appropriate comparisons to control flies, and yet occasionally these control experiments are not performed. Our results serve as an important reminder that careful background controls are critically important to the interpretation of experiments using genetically modified animals.

In this chapter I presented weak evidence that activating the OA-AL2i1 neuron may increase visual responses in VS cells. It remains unclear what contribution individual octopamine neurons make in modulating visual responses during flight, but based on anatomy, I expect that the visual system is modulated at multiple levels – octopaminergic processes innervate the optic lobes at the level of the medulla, the lobula, and the lobula plate. I hope that future experiments, bolstered by the rapidly developing set of genetic tools in *Drosophila*, will help build a more complete picture of the modulatory network that underlies the flight boost.

Chapter 4

Mechanosensory input and the flight boost

4.1 Introduction

Octopamine neurons appear to be responsible for the VS cell flight boost, and, based on anatomy, probably modulate many other parts of the visual system during flight. I showed that the octopamine neurons that project to the optic lobes become active during flight, but it remains unclear what drives this activity. During flight, these neurons may receive a central signal corresponding to the behavioral state, or they may also receive mechanosensory feedback, similar to what has been hypothesized to be the case in the octopaminergic, multimodal locust DCMD neuron (Rowell, 1971). In this chapter, I briefly explore the role of wind stimuli in the flight boost. I show, for the first time, that the visual responses of lobula plate tangential cells are modulated by mechanosensory stimuli.

4.2 Experimental procedures

All experimental procedures were performed as described in Chapter 2 with any exceptions listed below.

4.2.1 Animals

Animals were reared and prepared for experiments as outlined in Chapter 2. I made use of the following transgenic flies: *DB331-Gal4* (Scott et al., 2002, FBti0115113) and *UAS-2xEGFP* (Bloomington 6874). See Table 2.1 for complete genotypes of these flies.

4.2.2 Whole cell patch clamp recordings

I used electrodes with resistance of 4.8-7.4 MΩ. The average resting potential of cells after compensation for an experimentally-measured junction potential (-13mV) was -43.8mV. I injected 40-50 pA constant hyperpolarizing current into the cells prior to presentation of visual stimuli to aid with dye fills, which decreased the membrane potential by an average of -7.2mV (to -51.0 mV). The access resistance (R_{acc}) for all recordings was 31.1 +/- 8.6 MΩ S.D.. Any cells with R_{acc} greater than 50MΩ were excluded from our analysis. See Chapter 2 for additional recording methods.

4.2.3 Visual display and stimuli

I used the same LED display and sine-wave grating stimulus as described in Chapter 2. For the 1 Hz responses, I presented flies only with downward and upward 1Hz motion. I presented flies with 2 s of alternating upward and downward motion, with 8 s of a stationary mean luminance pattern in between trials. The pattern began motion at the same quadrant in the sine-wave pattern for each trial. 8 Hz responses were obtained from a subset of the data presented in Chapter 2 (flies for which 8 Hz wind stimuli responses existed - see Data Analysis and Statistics below).

4.2.4 Data analysis and statistics

As in Chapter 2, I applied a small puff of air directed towards the fly's head to initiate flight. I observed an increase in visual responses for approximately 20 s after a brief puff (or a short, ≤ 5, rapid set of puffs) was delivered to the fly in the absence of flight.

If no flight was initiated, visual responses during the 20 s after I applied a puff of air were included in the wind stimulus average. Any visual motion trials during which a puff was applied were omitted from this average. For each fly, I averaged across all of the post-wind stimulus averages to obtain a single measure of the wind stimulus effect on membrane potential. To aid in the direct comparison between air-induced and flight-induced visual boosts, only flies who had trials that qualified for the wind stimulus average and who also flew were included in this analysis. I characterized this effect at 1 and 8 Hz, speeds at which the VS cells show the largest response to motion and the largest flight boost, relatively.

4.3   Results

I noticed that after a brief air pulse, if a fly failed to initiate flight, its VS cell responses to visual motion still increased and remained elevated for approximately 20 s after the air pulse (Figure 4.1). This increase in response to motion decayed over time, but was otherwise reminiscent of the increase observed during flight. At 1 Hz, the increase in baseline-subtracted visual response was minimal during flight (0.26 mV, or 4.4%), but significant at 8 Hz (2.4 mV, or 70.5%), consistent with our previous results (Figures 4.2 and 4.3, see also Chapter 2, Figure 2.1C and D). However, VS cell responses to both 1 and 8 Hz motion were large after a wind stimulus - I observed increases of 2.3 mV (39.3%) and 2.1 mV (62.8%), relatively (Figures 4.2 and 4.3). Unlike during flight, the wind stimulus did not cause an increase in baseline membrane potential (Figures 4.3 and 4.4). These results show that a wind stimulus alone can induce a transient visual boost in VS cells in the absence of flight, independently of the baseline shift observed during flight.

4.4   Discussion

In this chapter, I presented evidence for a mechanosensory-induced visual boost in VS cells. In the absence of flight, a brief pulse of air is sufficient to induce an increase in
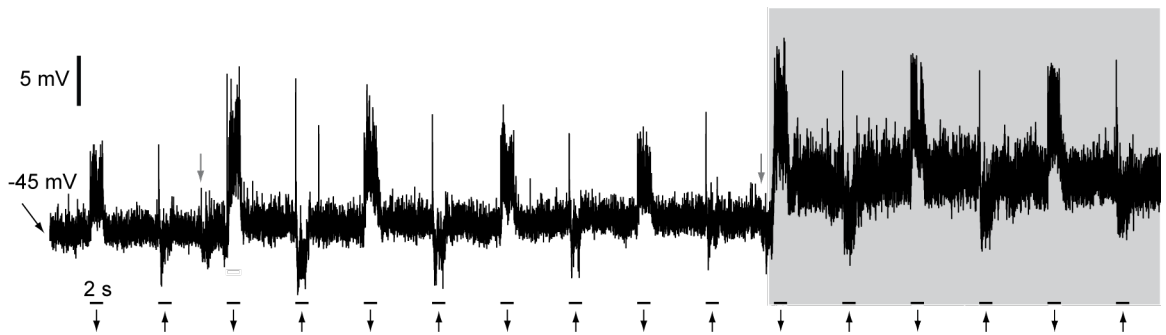
Figure 4.1: Wind stimulus induces a transient increase in VS cell response to visual motion. Example trace of one VS cell's response to visual motion before and after a brief pulse of air that did not elicit flight (left vertical arrow), followed by a pulse of air that elicits a flight bout (right vertical arrow, flight indicated by grey shaded region). Direction of motion is indicated by the black arrows. The average baseline membrane potential during quiescence is shown.
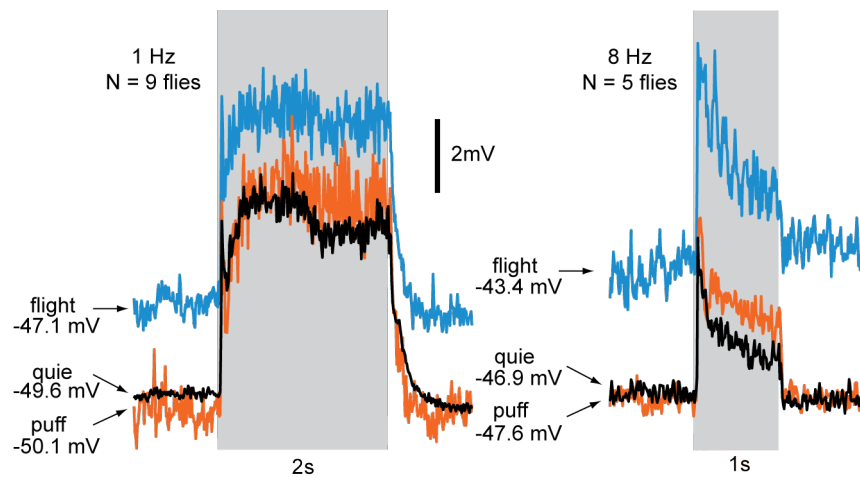
Figure 4.2: Average VS cell response to motion after a wind stimulus. Average visual response to 1 Hz (left) and 8 Hz (right) downward motion during flight (blue traces), after a wind stimulus that does not elicit flight ('puff', orange traces) and corresponding quiescent responses ('quie', black traces). The grey shaded region indicates when the visual stimulus was in motion. The average baseline membrane potential during the 1 s immediately before motion onset is shown for quiescence, post-wind stimulus and flight traces.
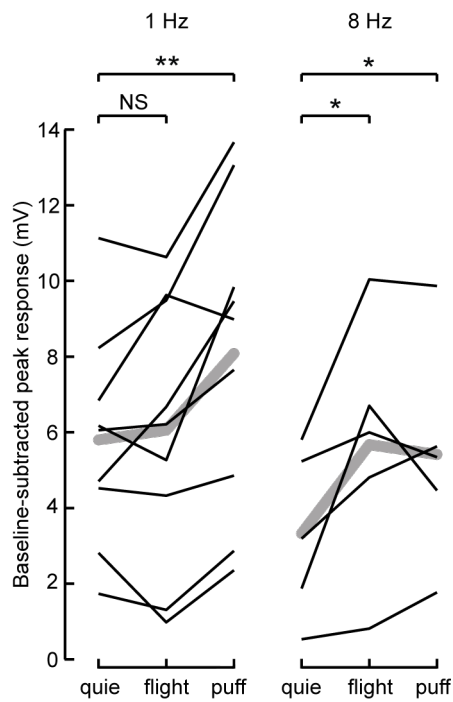
Figure 4.3: Wind stimulus generates an increase in individual fly average VS responses to visual motion. Average baseline-subtracted peak membrane potential responses to 1 or 8 Hz downward-moving sine wave grating. Asterisks indicate when responses during flight or after a wind stimuli ('puff') are significantly higher than quiescence ('quie'; paired Student's t-test). Single and double asterisks indicate significance at alpha = 0.05 and 0.01 respectively. NS indicates no significance at alpha <= 0.05.
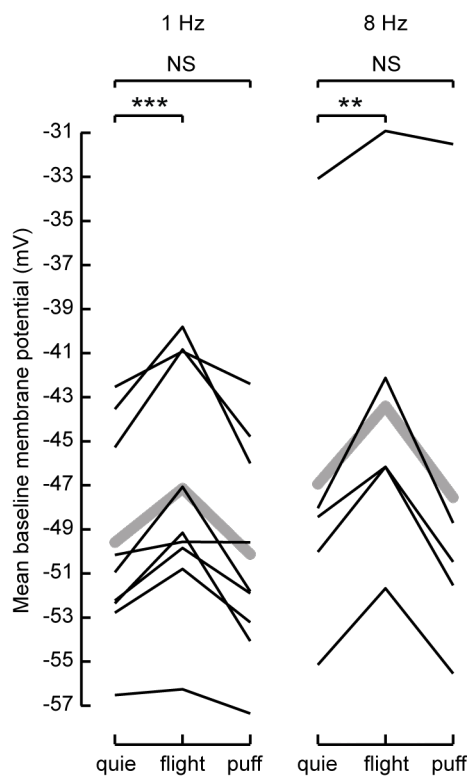
Figure 4.4: Baseline membrane potential does not change after wind stimulus. Average individual fly baseline membrane potential during quiescence ('quie'), flight and after a wind stimulus that does not elicit flight ('puff'). Average baseline membrane potential responses during the 1 s immediately before 1 or 8 Hz downward motion. Asterisks indicate when responses during flight or after a wind stimuli are significantly higher than quiescence (paired Student's t-test). Double and triple asterisks indicate significance at alpha = 0.01 and 0.001 respectively. NS indicates no significance at alpha <= 0.05.

response to motion reminiscent of that observed during flight. Similar to flight, this response decays within a few tens of seconds, but is not accompanied by the rapid upward shift in membrane potential observed during flight. These results suggest that a mechanosensory stimulus may underlie the flight boost. Maimon et al. (2010) showed that the flight boost can last for the duration of long (≥ 35 s), uninterrupted flight bouts in the absence of any air puffs, and so I believe it unlikely that this initial wind stimulus boost can explain the long-lasting increase in visual response to motion. However, the air puff I use to elicit flight may stimulate the same system that also responds to a mechanosensory stimulus present during flight, such as airflow over the antenna, halteres or the wings. This may explain why the boost is largest at the beginning of a flight (Supplementary Figure 3 in Maimon et al., 2010, see also example trace in Figure 4.1); in these experiments and in Maimon et al. (2010), all flight data presented were obtained from flights elicited using a wind stimulus because spontaneous flights are rare in this preparation. Future experiments could test this hypothesis by comparing the visual boost between flights elicited by a wind stimuli and flights elicited in the absence of any wind stimuli, for example with a visual expansion stimulus that triggers an escape reflex.

In Chapter 2, I showed that the flight boost is mediated by octopamine neurons, whereas the baseline shift is mediated by a second, unknown mechanism. The wind-induced boost I observe in non-flying flies suggests that one possible source of the flight boost is one or more octopamine neurons sensitive to mechanosensory stimuli. These neurons may receive continual mechanosensory stimuli during flight, and the slightly larger flight boost I observe at the beginning of flight may result from the relatively stronger air puff stimuli I deliver to elicit flight in this preparation. More experiments are necessary to determine if this is the case, and if so, what sensors could be contributing to this system. Our results are similar to findings in locust multimodal octopaminergic neurons (see Chapter 1, Section 1.3.1), however, and suggest that conserved mechanisms underlying flight modulation of the visual system exist.

Chapter 5

Conclusion

The octopamine orchestration hypothesis made explicit predictions about the role of octopamine neurons in regulating insect behavior. Sombati and Hoyle (1984) proposed that specific modulatory neurons were responsible for coordinating wide-scale changes in physiology that were necessary to elicit various behaviors, and that octopamine played such a role for flight. The fact that flies in which I presumably reduced the activity of all octopamine neurons still retained the ability to fly suggests that the original hypothesis, strictly interpreted, does not apply to *Drosophila*. Our results from Chapter 2 are also consistent with an earlier genetic study which demonstrated that octopamine null mutants are able to fly, albeit less robustly (Brembs et al., 2007). However, although octopamine may not be necessary for flight, our results are consistent with prior research in locusts suggesting that octopamine does play an important role in modulating physiology during flight. Our results show that a set of octopamine neurons in *Drosophila* with dense projections to the optic lobes increase in activity during flight. Based on previous anatomical studies, these neurons are likely to belong to the AL2 cluster (Busch et al., 2009) (also called G3a in Sinakevitch et al., 2005). The locust multimodal protocerebrum-medulla (PM) neurons, some of which have been shown to be octopaminergic, share remarkable anatomical similarity with these neurons (Stern et al., 1995). Further, the octopaminergic PM4 neuron appears to play a role in dishabituating the descending contralateral movement detector (DCMD; Bacon et al., 1995), which is involved in mediating startle reflexes (Pearson et al., 1980; Fotowat et al., 2011). The PM4 neuron is thought to

release octopamine in the optic lobes in response to a variety of novel stimuli and is presynaptic to the lobula giant motion detector, which then synapses onto the DCMD (Bacon et al., 1995, see also Section 1.3.1). This simple visual circuit probably plays a part in an arousal mechanism in the locust, but it remains to be determined what behavior triggers its activation, and ultimately what functional role it plays in the behavior of the animal. In the fruit fly, we now have evidence that a set of octopaminergic neurons that project to the optic lobes increase in activity during flight, and that they likely play a role in the behavioral modulation of visual motion responses in lobula plate tangential neurons. The similarities between the neurons believed to be involved in arousal mechanisms in locusts and the cells involved in the flight modulation that I examined in this thesis hint that there may exist conserved modulatory mechanisms mediated by octopamine neurons.

The role of neuromodulators in the crustacean stomatogastric ganglion (STG) has been particularly well characterized, and serves as another point of reference for our findings. Activity patterns in the STG are regulated by multiple modulators, and a single modulator is capable of eliciting entirely different responses from individual neurons depending on the expression of particular ion channels (Harris-Warrick et al., 1998). A few of these substances are known to be released onto the STG neuropil during specific behavioral states, but it remains unclear what role each one plays during different behaviors (Marder and Bucher, 2007). Octopamine has been shown to increase overall pyloric activity in the lobster STG and can induce two distinct, stable motor patterns depending on concentration (Flamm and Harris-Warrick, 1986a). Octopamine is thought to play a role in activity-dependent modulation in the STG, but to our knowledge, this has not been investigated, although endogenous action of serotonin has been explored (Katz et al., 1989). In the STG, and in other circuits across a variety of behaviors and organisms, it is thought that neuromodulators multiply the number of functions that the circuit can perform (Harris-Warrick and Marder, 1991). The fly brain has on the order of a hundred thousand neurons, yet is responsible for the coordination of a remarkable repertoire of complex behaviors. It seems possible that insects, like crustaceans, may employ neuromodulators to increase the functional

capacity of their relatively small brains.

Although I have identified a set of octopamine neurons with projections in the optic lobes that are likely responsible for mediating the flight boost, the precise site of modulation is still unknown. The VS cells may be directly modulated, upstream cells could be the target of the octopaminergic input, or a combination of direct and indirect modulation may occur. These alternative hypotheses will require a detailed investigation of the location and action of octopamine receptors in the optic lobes. However, recent studies in hoverflies (de Haan et al., 2012) and blowflies (Rien et al., 2012) suggest that the action of octopamine, at least in part, may be presynaptic to the VS cells. It is also unclear how octopamine neurons become activated during flight. Based on the observation that an air puff that does not induce flight can alone induce elevated visual responses (Chapter 4), it seems possible that a wind-sensitive mechanosensory input may contribute to the flight boost. Careful experiments to determine which sensory modalities are involved will be needed to resolve this. Furthermore, using combinatorial techniques (see Chapter 3), we can begin to investigate whether the octopamine neurons act in concert, or if individual octopamine neurons have distinct roles in mediating changes in the optic lobes during flight.

Our results provide evidence that the flight boost observed in VS cells is mediated by octopamine neurons, but the origin of the baseline shift is still unclear. Neck motor neurons and descending interneurons, which integrate information from a number of sensory modalities, are the post-synaptic targets of the LPTCs. Based on anatomical and electrophysiological evidence in blowflies, the VS cells appear to be electrically coupled to both of these types of interneurons (Wertz et al., 2008; Haag et al., 2007; Wertz et al., 2012). The baseline shift observed in VS cells could be the result of excitation of these downstream neurons by rapid mechanosensory input, from the halteres for example. Alternatively, a central command signal may excite the VS cells indirectly via this electrical coupling to descending interneurons. In *Drosophila*, I can test these hypotheses starting by using a Gal4 driver line I recently found that labels a subset of VS cells and a descending interneuron that displays characteristics similar to the DNOVS cells identified in *Calliphora* (data not shown). I can perform dual

recordings to determine first whether the VS cells and this descending interneuron are indeed electrically coupled. Next I hope to identify any flight effects in this downstream neuron, then characterize information transfer between the two cell types during quiescence and flight. In addition to investigating the source of the baseline shift, these future experiments may lead towards insights in the downstream effects of the flight boost, as well as a fuller understanding of the role VS cells play in different behaviors.

In a set of preliminary experiments in collaboration with Floris van Breugel and Bettina Schnell, we have begun to investigate the role of the flight boost observed in VS cells and of octopamine neurons in regulating flight behavior. Briefly, we investigated the effect of genetically silencing octopamine neurons by expressing Kir2.1 in octopamine neurons using the *Tdc2-Gal4* driver (see Figure 5.1B for expression pattern in the brain and thoracic ganglia), in freely flying flies. We allowed flies to fly freely in a wind tunnel and presented them with regressive motion stimuli. Moving gratings of different temporal frequencies were projected on the side of the wind tunnel, and we recorded 3-D flight trajectories before, during, and after these visual stimuli (Figure 5.1A). We found that flies whose octopamine neurons were inactivated accelerated less than the two corresponding parental strains (Figure 5.2A). Male and female flies within each genotype performed similarly, suggesting that this effect was probably not caused by the known egg-laying deficit phenotype in octopamine null females (females are unable to lay eggs, and at maturity, are typically large due to egg retention). Furthermore, flies whose octopamine neurons were inactivated showed normal flight speeds (Figure 5.2E) and accelerations (Figure 5.2F) in the absence of motion stimuli, suggesting that our genetic manipulation did not cause a gross motor defect. We believe it is more likely that our manipulation induced a defect in the gain control system regulating flight behavior. Although we cannot be sure that these effects are mediated by the LPTC network, this hypothesis is supported by recent experiments indicating that octopamine alters the gain of neurons within this system (Suver et al., 2012; Maimon et al., 2010; Longden and Krapp, 2009, 2010; Jung et al., 2011). This experiment suggests that the flight boost we observe in VS
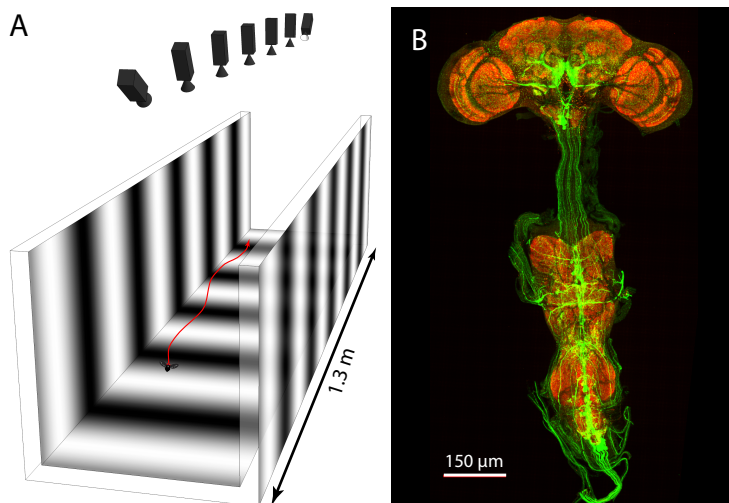
Figure 5.1: Free flight behavioral apparatus and Gal4 driver line expression. (A) Wind tunnel in which the experiments were performed, with a properly scaled representation of the 4.2 m-1 spatial frequency used during the experiments. (B) Confocal image of a *Drosophila* brain and thoracic ganglion showing the GFP labeled octopamine neurons (green), which we genetically silenced with Kir2.1 using the *Tdc2-Gal4* driver line.

cells may be indicative of a system-wide gain modulation mechanism mediated by octopamine neurons during flight, and is the first evidence that points toward the behavioral significance of the flight boost.

The functional relevance of the flight effects observed in VS cells remains to be fully characterized, however. The flight boost might serve as a general arousal mechanism that provides the fly with a heightened ability to process relevant information during flight. Alternatively, the fly might conserve energy by maintaining a lower state of activity in the visual system at rest, increasing the gain only when needed (Niven and Laughlin, 2008). The results described in Chapter 2 implicate octopamine neurons in producing one of the two most salient flight effects observed in VS cells, taking a first step towards understanding the functional relevance and mechanisms of the flight modulation. Furthermore, our preliminary free flight experiments provide evidence that these neurons are involved in a flight speed control mechanism. More refined genetic reagents will help to identify which octopamine neurons are involved in this gain control, and more precisely the define the role of LPTCs and other neurons involved in this pathway. Although these details remain unclear, we have provided
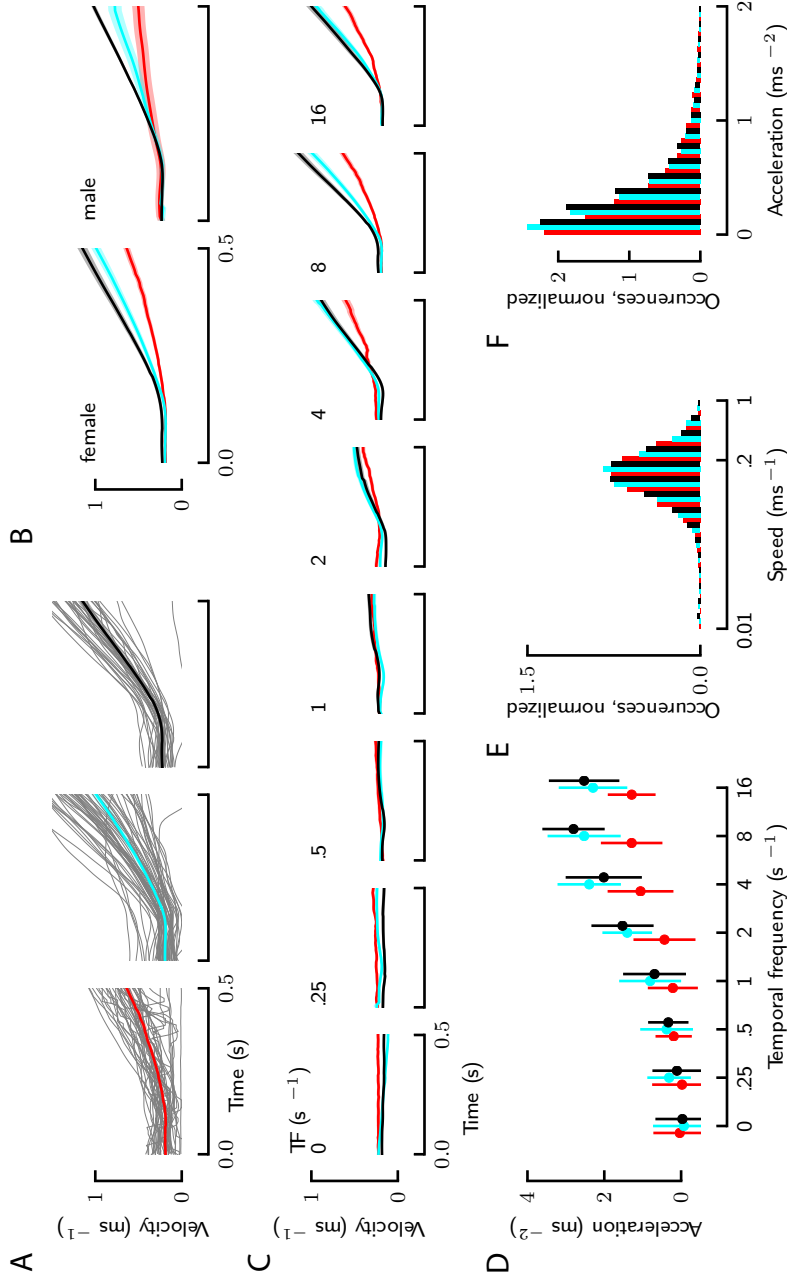
Figure 5.2: Octopamine null flies respond to regressive visual motion during free flight with lower accelerations than wild type flies. (A) Raw (gray) and mean (colored) velocity *vs.* time responses to regressive visual motion with a temporal frequency of 8 Hz for flies with inactivated octopamine neurons (red), and the parental controls (blue, *Tdc2-Gal4* and black, *UAS-Kir2.1-eGFP*). We use consistent colors in subsequent panels. (B) Mean velocity responses to regressive visual motion stimulus for males and females. (C) Mean velocity responses to regressive motion at different temporal frequencies. (D) Acceleration responses to regressive motion *vs.* temporal frequency (mean ± std dev). (E) Histogram of steady state velocity in the absence of regressive motion stimuli. (F) Baseline acceleration responses in the absence of regressive motion stimuli. In (B) and (C) standard error for each condition is shown in lighter respective colors.

the first functional implication of the flight effects observed in the visual system of *Drosophila*.

Bibliography

Adamo, S., Linn, C., and Hoy, R. (1995). The role of neurohormonal octopamine during 'fight or flight' behaviour in the field cricket *Gryllus bimaculatus*. *J Exp Biol*, 198(8):1691–1700.

Alekseyenko, O. V., Chan, Y.-B., Li, R., and Kravitz, E. A. (2013). Single dopaminergic neurons that modulate aggression in *Drosophila*. *Proceedings of the National Academy of Sciences*, 110(15):6151–6156.

Andermann, M. L., Kerlin, A. M., Roumis, D. K., Glickfeld, L. L., and Reid, R. C. (2011). Functional specialization of mouse higher visual cortical areas. *Neuron*, 72(6):1025–39.

Autrum, H. (1958). Electrophysiological analysis of the visual systems in insects. *Exp Cell Res*, 14(Suppl 5):426.

Bacon, J. P., Thompson, K. S., and Stern, M. (1995). Identified octopaminergic neurons provide an arousal mechanism in the locust brain. *J Neurophysiol*, 74(6):2739–43.

Baines, R. A., Uhler, J. P., Thompson, A., Sweeney, S. T., and Bate, M. (2001). Altered electrical properties in *Drosophila* neurons developing without synaptic transmission. *J Neurosci*, 21(5):1523–1531.

Bargmann, C. I. (2012). Beyond the connectome: How neuromodulators shape neural circuits. *BioEssays*, 34(6):458–465.

Bausenwein, B., Dittrich, A., and Fischbach, K.-F. (1992). The optic lobe of *Drosophila melanogaster*. *Cell Tissue Res*, 267(1):17–28.

Bicker, G., Menzel, R., et al. (1989). Chemical codes for the control of behaviour in arthropods. *Nature*, 337(6202):33–39.

Blondeau, J. and Heisenberg, M. (1982). The three-dimensional optomotor torque system of *Drosophila melanogaster*. *J Comp Physiol*, 145(3):321–329.

Borst, A., Egelhaaf, M., and Haag, J. (1995). Mechanisms of dendritic integration underlying gain control in fly motion-sensitive interneurons. *J Comp Neurosci*, 2(1):5–18.

Borst, A. and Haag, J. (2002). Neural networks in the cockpit of the fly. *J Comp Physiol A*, 188(6):419–37.

Braitenberg, V. (1972). Periodic structures and structural gradients in the visual ganglia of the fly. In *Information Processing in the Visual Systems of Arthropods*, pages 3–15. Springer.

Brembs, B., Christiansen, F., Pfluger, H. J., and Duch, C. (2007). Flight initiation and maintenance deficits in flies with genetically altered biogenic amine levels. *J Neurosci*, 27(41):11122–31.

Buchner, E. (1976). Elementary movement detectors in an insect visual system. *Biol Cybern*, 24(2):85–101.

Buchner, E. (1984). Behavioural analysis of spatial vision in insects. In *Photoreception and vision in invertebrates*, pages 561–621. Springer.

Buchner, E., Buchner, S., and Bülthoff, I. (1984). Deoxyglucose mapping of nervous activity induced in *Drosophila* brain by visual movement. 1. Wildtype. *J Comp Physiol A*, 155(4):471–483.

Burrows, M. (1996). *The Neurobiology of an Insect Brain*. Oxford University Press, New York.

Busch, S., Selcho, M., Ito, K., and Tanimoto, H. (2009). A map of octopaminergic neurons in the *Drosophila brain*. *J Comp Neurol*, 513(6):643–67.

Cajal, R. Y. and Sanchez, D. (1915). Contribucion al conocimiento de los centros nerviosos de los insectos. Parte 1. Retina y centros opticos. *Trab Lab Invest Bio Univ Madrid*, 13:1–168.

Chiappe, M. E., Seelig, J. D., Reiser, M. B., and Jayaraman, V. (2010). Walking modulates speed sensitivity in *Drosophila* motion vision. *Curr Biol*, 20(16):1470–5.

Clark, D. A., Bursztyn, L., Horowitz, M. A., Schnitzer, M. J., and Clandinin, T. R. (2011). Defining the computational structure of the motion detector in *Drosophila*. *Neuron*, 70(6):1165–1177.

Coyne, J. A., Boussy, I. A., Prout, T., Bryant, S. H., Jones, J., and Moore, J. A. (1982). Long-distance migration of *Drosophila*. *Amer Nat*, 119(4):589–595.

Davis, R. L. (2005). Olfactory memory formation in *Drosophila*: from molecular to systems neuroscience. *Annu Rev Neurosci*, 28:275–302.

de Haan, R., Lee, Y. J., and Nordstrom, K. (2012). Octopaminergic modulation of contrast sensitivity. *Front Integr Neurosci*, 6:55.

Dvorak, D. R., Bishop, L. G., and Eckert, H. E. (1975). On the identification of movement detectors in the fly optic lobe. *J Comp Physiol*, 100(1):5–23.

Eichner, H., Joesch, M., Schnell, B., Reiff, D. F., and Borst, A. (2011). Internal structure of the fly elementary motion detector. *Neuron*, 70(6):1155–1164.

Elyada, Y. M., Haag, J., and Borst, A. (2013). Dendritic end inhibition in large-field visual neurons of the fly. *J Neurosci*, 33(8):3659–3667.

Erspamer, V. (1948). Active substances in the posterior salivary glands of octopoda. ii. Tyramine and Octopamine (Oxyoctopamine). *Acta Pharmacol Toxicol*, 4(3-4):224–247.

Evans, P. D. and Maqueira, B. (2005). Insect octopamine receptors: a new classification scheme based on studies of cloned *Drosophila* G-protein coupled receptors. *Invert Neurosci*, 5(3-4):111–8.

Fayyazuddin, A. and Dickinson, M. H. (1996). Haltere afferents provide direct, electrotonic input to a steering motor neuron in the blowfly, *Calliphora*. *J Neurosci*, 16(16):5225–5232.

Flamm, R. and Harris-Warrick, R. (1986a). Aminergic modulation in lobster stomatogastric ganglion. I. effects on motor pattern and activity of neurons within the pyloric circuit. *J Neurophysiol*, 55(5):847–865.

Flamm, R. and Harris-Warrick, R. (1986b). Aminergic modulation in lobster stomatogastric ganglion. II. target neurons of dopamine, octopamine, and serotonin within the pyloric circuit. *J Neurophysiol*, 55(5):866–881.

Fotowat, H., Harrison, R. R., and Gabbiani, F. (2011). Multiplexing of motor information in the discharge of a collision detecting neuron during escape behaviors. *Neuron*, 69(1):147–58.

Fox, J. and Daniel, T. (2008). A neural basis for gyroscopic force measurement in the halteres of *Holorusia*. *J Comp Physiol A*, 194(10):887–897.

Franz, M. O. and Krapp, H. G. (2000). Wide-field, motion-sensitive neurons and matched filters for optic flow fields. *Biol Cybern*, 83(3):185–197.

Geiger, G. and Nassel, D. R. (1981). Visual orientation behaviour of flies after selective laser beam ablation of interneurones. *Nature*, 293(5831):398–9.

Getting, P. A. (1989). Emerging principles governing the operation of neural networks. *Ann Rev Neurosci*, 12(1):185–204.

Goaillard, J.-M., Schulz, D. J., Kilman, V. L., and Marder, E. (2004). Octopamine modulates the axons of modulatory projection neurons. *J Neurosci*, 24(32):7063–7073.

Goodman, L. J. (1970). The structure and function of the insect dorsal ocellus. *Adv Insect Physiol*, 7:97–195.

Goosey, M. and Candy, D. (1980). The D-octopamine content of the haemolymph of the locust, *Schistocerca americana gregaria* and its elevation during flight. *Insect Biochem*, 10(4):393–397.

Gronenberg, W. and Strausfeld, N. J. (1990). Descending neurons supplying the neck and flight motor of diptera: physiological and anatomical characteristics. *J Comp Neurol*, 302(4):973–991.

Guizar-Sicairos, M., Thurman, S. T., and Fienup, J. R. (2008). Efficient subpixel image registration algorithms. *Opt Lett*, 33(2):156–158.

Haag, J. and Borst, A. (2004). Neural mechanism underlying complex receptive field properties of motion-sensitive interneurons. *Nat Neurosci*, 7(6):628–634.

Haag, J. and Borst, A. (2005). Dye-coupling visualizes networks of large-field motion-sensitive neurons in the fly. *J Comp Physiol A*, 191(5):445–454.

Haag, J., Wertz, A., and Borst, A. (2007). Integration of lobula plate output signals by DNOVS1, an identified premotor descending neuron. *J Neurosci*, 27(8):1992–2000.

Haag, J., Wertz, A., and Borst, A. (2010). Central gating of fly optomotor response. *Proc Natl Acad Sci*, 107(46):20104–20109.

Hamada, F. N., Rosenzweig, M., Kang, K., Pulver, S. R., Ghezzi, A., Jegla, T. J., and Garrity, P. A. (2008). An internal thermal sensor controlling temperature preference in *Drosophila*. *Nature*, 454(7201):217–220.

Harris-Warrick, R. M., Johnson, B. R., Peck, J. H., Kloppenburg, P., Ayali, A., and Skarbinski, J. (1998). Distributed effects of dopamine modulation in the crustacean pyloric network. *Ann N Y Acad Sci*, 860:155–67.

Harris-Warrick, R. M. and Marder, E. (1991). Modulation of neural networks for behavior. *Annu Rev Neurosci*, 14:39–57.

Hassenstein, B. and Reichardt, W. (1956). Systemtheoretische Analyse der Zeit, Reihenfolgen und Vorzeichenauswertung bei der Bewegungsperzeption des Rüsselkäfers *Chlorophanus*. *Z. Naturforsch*, 11b:513–524.

Hausen, K. (1976). Functional characterization and anatomical identification of motion sensitive neurons in the lobula plate of the blowfly *Calliphora erythrocephala*. *Z Naturforsch*, 31:629–633.

Hausen, K. (1984). The lobula-complex of the fly: structure, function and significance in visual behaviour. In *Photoreception and vision in invertebrates*, pages 523–559. Springer.

Hausen, K. and Wehrhahn, C. (1983). Microsurgical lesion of horizontal cells changes optomotor yaw responses in the blowfly *Calliphora erythrocephala*. *Proc Royal Soc Lond [Biol]*, 219(1215):211–216.

Hausen, K. and Wehrhahn, C. (1990). Neural circuits mediating visual flight control in flies. II. separation of two control systems by microsurgical brain lesions. *J Neurosci*, 10(1):351–360.

Heisenberg, M., Wolf, R., et al. (1984). *Vision in* Drosophila. *Genetics of microbehaviour.* Springer Verlag.

Heisenberg, M., Wonneberger, R., and Wolf, R. (1978). optomotor-blind^{H31} - a *Drosophila* mutant of the lobula plate giant neurons. *J Comp Physiol*, 124(4):287–296.

Hengstenberg, R. (1977). Spike responses of 'non-spiking' visual interneurone. *Nature*, 270:338–340.

Hengstenberg, R. (1991). Gaze control in the blowfly *Calliphora*: a multisensory, two-stage integration process. In *Seminars in Neuroscience*, volume 3, pages 19–29. Elsevier.

Hengstenberg, R., Hausen, K., and Hengstenberg, B. (1982). The number and structure of giant vertical cells (VS) in the lobula plate of the blowfly *Calliphora erythrocephala*. *J Comp Physiol*, 149(2):163–177.

Hoyer, S. C., Eckart, A., Herrel, A., Zars, T., Fischer, S. A., Hardie, S. L., and Heisenberg, M. (2008). Octopamine in male aggression of *Drosophila*. *Curr Biol*, 18(3):159–167.

Huston, S. J. and Krapp, H. G. (2008). Visuomotor transformation in the fly gaze stabilization system. *PLoS Biol*, 6(7):e173.

Huston, S. J. and Krapp, H. G. (2009). Nonlinear integration of visual and haltere inputs in fly neck motor neurons. *J Neurosci*, 29(42):13097–105.

Inagaki, H. K., Ben-Tabou de Leon, S., Wong, A. M., Jagadish, S., Ishimoto, H., Barnea, G., Kitamoto, T., Axel, R., and Anderson, D. J. (2012). Visualizing neuromodulation in vivo: TANGO-mapping of dopamine signaling reveals appetite control of sugar sensing. *Cell*, 148(3):583–595.

Ito, K., Suzuki, K., Estes, P., Ramaswami, M., Yamamoto, D., and Strausfeld, N. J. (1998). The organization of extrinsic neurons and their implications in the functional roles of the mushroom bodies in *Drosophila melanogaster* meigen. *Learn Memory*, 5(1):52–77.

Joesch, M., Plett, J., Borst, A., and Reiff, D. F. (2008). Response properties of motion-sensitive visual interneurons in the lobula plate of *Drosophila melanogaster*. *Curr Biol*, 18(5):368–74.

Joesch, M., Schnell, B., Raghu, S. V., Reiff, D. F., and Borst, A. (2010). ON and OFF pathways in *Drosophila* motion vision. *Nature*, 468(7321):300–304.

Johns, D. C., Marx, R., Mains, R. E., O'Rourke, B., and Marbán, E. (1999). Inducible genetic suppression of neuronal excitability. *J Neurosci*, 19(5):1691–1697.

Jösch Krotki, M. A. (2009). *Lobula Plate Tangential Cells in Drosophila melanogaster.* PhD thesis, lmu.

Jung, S. N., Borst, A., and Haag, J. (2011). Flight activity alters velocity tuning of fly motion-sensitive neurons. *J Neurosci*, 31(25):9231–7.

Karmeier, K., van Hateren, J., Kern, R., and Egelhaaf, M. (2006). Encoding of naturalistic optic flow by a population of blowfly motion-sensitive neurons. *J Neurophysiol*, 96(3):1602–1614.

Katz, P. S., Eigg, M. H., and Harris-Warrick, R. M. (1989). Serotonergic/cholinergic muscle receptor cells in the crab stomatogastric nervous system. I. identification and characterization of the gastropyloric receptor cells. *J Neurophysiol*, 62(2):558–70.

Kern, R., van Hateren, J., Michaelis, C., Lindemann, J. P., and Egelhaaf, M. (2005). Function of a fly motion-sensitive neuron matches eye movements during free flight. *PLoS Biol*, 3(6):e171.

Kosakai, K., Satoh, K., and Yoshino, M. (2008). Octopaminergic modulation of the single Ca^{2+} channel currents in kenyon cells isolated from the mushroom body of the cricket brain. *J Insect Physiol*, 54(12):1479–1486.

Krapp, H. G., Hengstenberg, B., and Hengstenberg, R. (1998). Dendritic structure and receptive-field organization of optic flow processing interneurons in the fly. *J Neurophysiol*, 79(4):1902–1917.

Krapp, H. G. and Hengstenberg, R. (1996). Estimation of self-motion by optic flow processing in single visual interneurons. *Nature*, 384(6608):463–6.

Kravitz, E. A. and Huber, R. (2003). Aggression in invertebrates. *Curr Opin Neurobiol*, 13(6):736–743.

Longden, K. D. and Krapp, H. G. (2009). State-dependent performance of optic-flow processing interneurons. *J Neurophysiol*, 102(6):3606–18.

Longden, K. D. and Krapp, H. G. (2010). Octopaminergic modulation of temporal frequency coding in an identified optic flow-processing interneuron. *Front Syst Neurosci*, 4:153.

Maimon, G., Straw, A. D., and Dickinson, M. H. (2010). Active flight increases the gain of visual motion processing in *Drosophila*. *Nat Neurosci*, 13(3):393–9.

Marder, E. (2012). Neuromodulation of neuronal circuits: back to the future. *Neuron*, 76(1):1–11.

Marder, E. and Bucher, D. (2007). Understanding circuit dynamics using the stomatogastric nervous system of lobsters and crabs. *Annu Rev Physiol*, 69:291–316.

Marder, E. and Calabrese, R. L. (1996). Principles of rhythmic motor pattern generation. *Physiol Rev*, 76(3):687–717.

Matheson, T. (1997). Octopamine modulates the responses and presynaptic inhibition of proprioceptive sensory neurones in the locust *Schistocerca gregaria*. *J Exp Biol*, 200(9):1317–1325.

Menzel, R. and Muller, U. (1996). Learning and memory in honeybees: from behavior to neural substrates. *Annu Rev Neurosci*, 19(1):379–404.

Milde, J., Seyan, H., and Strausfeld, N. (1987). The neck motor system of the fly *Calliphora erythrocephala*. *J Comp Physiol A*, 160(2):225–238.

Monastirioti, M., Linn, C. E., J., and White, K. (1996). Characterization of *Drosophila* tyramine beta-hydroxylase gene and isolation of mutant flies lacking octopamine. *J Neurosci*, 16(12):3900–11.

Moran, J. and Desimone, R. (1985). Selective attention gates visual processing in the extrastriate cortex. *Science*, 229(4715):782–784.

Nalbach, G. (1993). The halteres of the blowfly calliphora. *Journal of Comparative Physiology A*, 173(3):293–300.

Nässel, D. R. and Hagberg, M. (1985). Ocellar interneurones in the blowfly *Calliphora erythrocephala*: Morphology and central projections. *Cell Tissue Res*, 242(2):417–426.

Niell, C. M. and Stryker, M. P. (2010). Modulation of visual responses by behavioral state in mouse visual cortex. *Neuron*, 65(4):472–9.

Niven, J. E. and Laughlin, S. B. (2008). Energy limitation as a selective pressure on the evolution of sensory systems. *J Exp Biol*, 211(Pt 11):1792–804.

Orchard, I., Ramirez, J. M., and Lange, A. B. (1993). A multifunctional role for octopamine in locust flight. *Annu Rev Entomol*, 38(1):227–249.

Parsons, M. M., Krapp, H. G., and Laughlin, S. B. (2010). Sensor fusion in identified visual interneurons. *Curr Biol*, 20(7):624–628.

Pearson, K. G., Heitler, W. J., and Steeves, J. D. (1980). Triggering of locust jump by multimodal inhibitory interneurons. *J Neurophysiol*, 43(2):257–78.

Pierantoni, R. (1973). An observation on the giant fibre posterior optic tract in the fly. *Biokybernetic, Leipzig*, 5(1):157–163.

Pringle, J. W. S. (1948). The gyroscopic mechanism of the halteres of *Diptera*. *Phil Trans R Soc London [Biol]*, pages 347–384.

Ramirez, J. M. and Orchard, I. (1990). Octopaminergic modulation of the forewing stretch-receptor in the locust *Locusta migratoria*. *J Exp Biol*, 149(1):255–279.

Ramirez, J.-M. and Pearson, K. G. (1991). Octopaminergic modulation of interneurons in the flight system of the locust. *J Neurophysiol*, 66(5):1522–1537.

Rein, K., Zöckler, M., Mader, M. T., Grübel, C., and Heisenberg, M. (2002). The *Drosophila* standard brain. *Curr Biol*, 12(3):227–231.

Reiser, M. B. and Dickinson, M. H. (2008). A modular display system for insect behavioral neuroscience. *J Neurosci Methods*, 167(2):127–39.

Rien, D., Kern, R., and Kurtz, R. (2012). Octopaminergic modulation of contrast gain adaptation in fly visual motion-sensitive neurons. *Eur J Neurosci*.

Roeder, T. (1999). Octopamine in invertebrates. *Prog in Neurobiol*, 59(5):533–561.

Rowell, C. F. (1971). Variable responsiveness of a visual interneurone in the free-moving locust, and its relation to behaviour and arousal. *J Exp Biol*, 55(3):727–747.

Schnell, B., Raghu, S. V., Nern, A., and Borst, A. (2012). Columnar cells necessary for motion responses of wide-field visual interneurons in *Drosophila*. *J Comp Physiol A*, 198(5):389–395.

Schuppe, H. and Hengstenberg, R. (1993). Optical properties of the ocelli of *Calliphora erythrocephala* and their role in the dorsal light response. *J Comp Physiol A*, 173(2):143–149.

Schwaerzel, M., Monastirioti, M., Scholz, H., Friggi-Grelin, F., Birman, S., and Heisenberg, M. (2003). Dopamine and octopamine differentiate between aversive and appetitive olfactory memories in *Drosophila*. *J Neurosci*, 23(33):10495–10502.

Scott, E. K., Raabe, T., and Luo, L. (2002). Structure of the vertical and horizontal system neurons of the lobula plate in *Drosophila*. *J Comp Neurol*, 454(4):470–81.

Siegelbaum, S. A. and Tsien, R. W. (1983). Modulation of gated ion channels as a mode of transmitter action. *Trends Neurosci*, 6(8):307–313.

Sinakevitch, I., Niwa, M., and Strausfeld, N. J. (2005). Octopamine-like immunoreactivity in the honey bee and cockroach: comparable organization in the brain and subesophageal ganglion. *J Comp Neurol*, 488(3):233–54.

Sinakevitch, I. and Strausfeld, N. J. (2006). Comparison of octopamine-like immunoreactivity in the brains of the fruit fly and blow fly. *J Comp Neurol*, 494(3):460–75.

Sombati, S. and Hoyle, G. (1984). Generation of specific behaviors in a locust by local release into neuropil of the natural neuromodulator octopamine. *J Neurobiol*, 15(6):481–506.

Stern, M., Thompson, K. S. J., Zhou, P., Watson, D. G., Midgley, J. M., Gewecke, M., and Bacon, J. P. (1995). Octopaminergic neurons in the locust brain: morphological, biochemical and electrophysiological characterization of potential modulators of the visual system. *J Comp Physiol A*, 177(5):611–625.

Strausfeld, N. and Bassemir, U. (1985). Lobula plate and ocellar interneurons converge onto a cluster of descending neurons leading to neck and leg motor neuropil in *Calliphora erythrocephala*. *Cell Tissue Res*, 240(3):617–640.

Strausfeld, N., Bassemir, U., Singh, R., and Bacon, J. (1984). Organizational principles of outputs from dipteran brains. *J Insect Physiol*, 30(1):73–93.

Strausfeld, N. and Seyan, H. (1985). Convergence of visual, haltere, and prosternai inputs at neck motor neurons of *Calliphora erythrocephala*. *Cell Tissue Res*, 240(3):601–615.

Strausfeld, N., Seyan, H., and Milde, J. (1987). The neck motor system of the fly *Calliphora erythrocephala*. *J Comp Physiol A*, 160(2):205–224.

Strausfeld, N. J. (1976). *Atlas of an insect brain*. Springer-Verlag Berlin, Heidelberg, New York.

Straw, A. and Dickinson, M. (2009). Motmot, an open-source toolkit for realtime video acquisition and analysis. *Source Code Biol Med*, 4.

Suver, M. P., Mamiya, A., and Dickinson, M. H. (2012). Octopamine neurons mediate flight-induced modulation of visual processing in *Drosophila*. *Curr Biol*.

Sweeney, S. T., Broadie, K., Keane, J., Niemann, H., and O'Kane, C. J. (1995). Targeted expression of tetanus toxin light chain in *Drosophila* specifically eliminates synaptic transmission and causes behavioral defects. *Neuron*, 14(2):341–351.

Taghert, P. H. and Nitabach, M. N. (2012). Peptide neuromodulation in invertebrate model systems. *Neuron*, 76(1):82–97.

Tian, L., Hires, S. A., Mao, T., Huber, D., Chiappe, M. E., Chalasani, S. H., Petreanu, L., Akerboom, J., McKinney, S. A., Schreiter, E. R., Bargmann, C. I., Jayaraman, V., Svoboda, K., and Looger, L. L. (2009). Imaging neural activity in worms, flies and mice with improved gcamp calcium indicators. *Nat Methods*, 6(12):875–81.

Treue, S. and Maunsell, J. H. R. (1996). Attentional modulation of visual motion processing in cortical areas MT and MST. *Nature*, 382(6591):539–541.

Venken, K. J., Simpson, J. H., and Bellen, H. J. (2011). Genetic manipulation of genes and cells in the nervous system of the fruit fly. *Neuron*, 72(2):202–230.

von Philipsborn, A. C., Liu, T., Yu, J. Y., Masser, C., Bidaye, S. S., and Dickson, B. J. (2011). Neuronal control of *Drosophila* courtship song. *Neuron*, 69(3):509–522.

Weir, P. T. and Suver, M. P. (2013). From dendritic compartments to neuronal networks: A multilevel analysis of motion vision. *J Neurosci*, 33(24):9876–9878.

Wertz, A., Borst, A., and Haag, J. (2008). Nonlinear integration of binocular optic flow by DNOVS2, a descending neuron of the fly. *J Neurosci*, 28(12):3131–3140.

Wertz, A., Haag, J., and Borst, A. (2012). Integration of binocular optic flow in cervical neck motor neurons of the fly. *J Comp Physiol A*, 198(9):655–668.

Wilson, R. I., Turner, G. C., and Laurent, G. (2004). Transformation of olfactory representations in the *Drosophila* antennal lobe. *Sci Signal*, 303(5656):366.

Zhou, C., Rao, Y., and Rao, Y. (2008). A subset of octopaminergic neurons are important for *Drosophila* aggression. *Nat Neurosci*, 11(9):1059–1067.